

An aerial photograph of the Diamond Light Source facility. The central feature is a large, circular, silver-colored building with a segmented roof, resembling a giant donut. This is the synchrotron ring. To the left of the ring is a smaller, white, multi-story building. In the background, there are green fields, trees, and a road network. The overall scene is a mix of industrial and rural landscapes.

# Small Angle X-ray Scattering

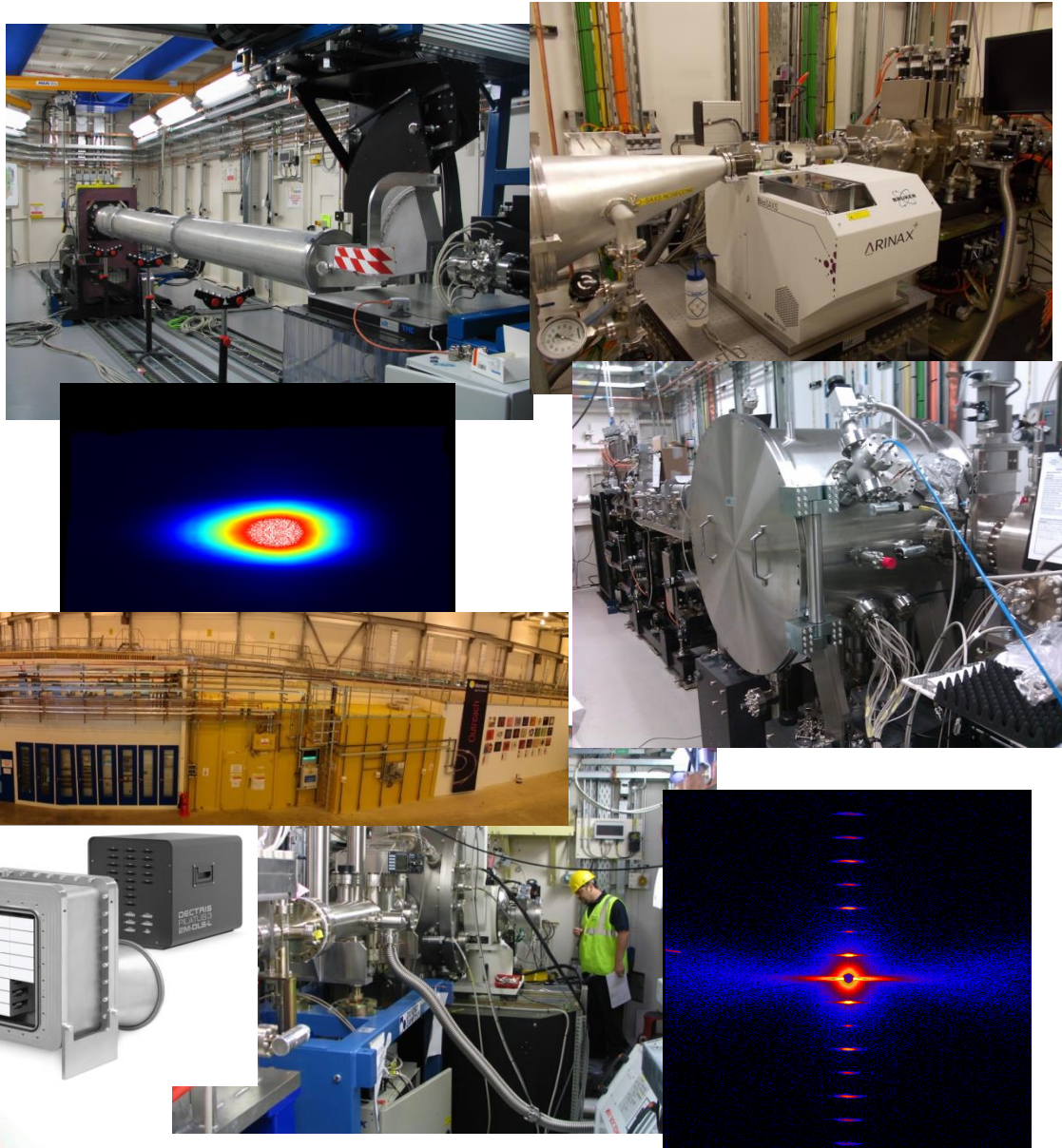
The last resort of the desperate!

Nick Terrill – Principal Beamline Scientist, Scattering, Diamond

# SAXS at Diamond

## Beamline Progress and Science highlights

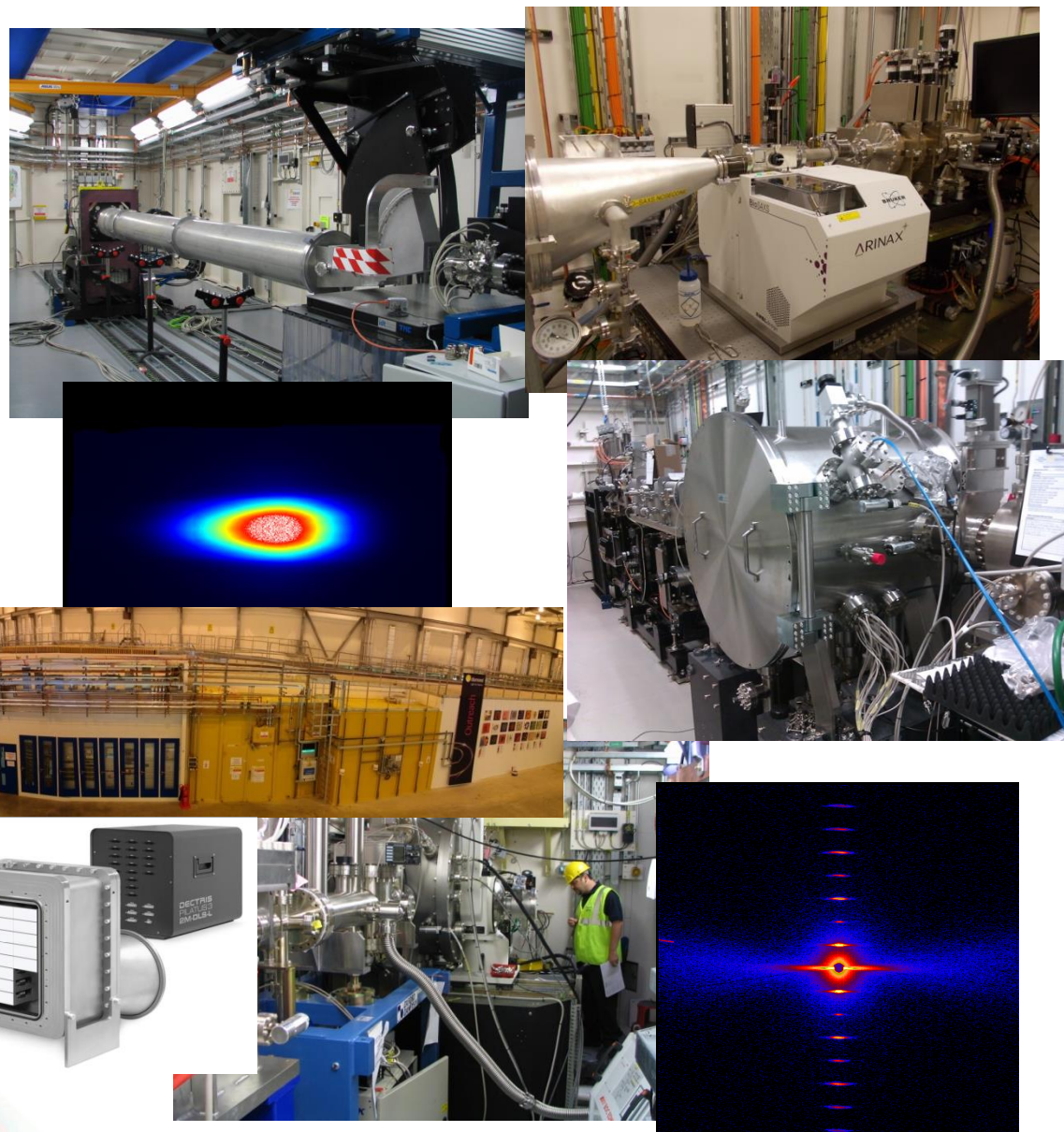
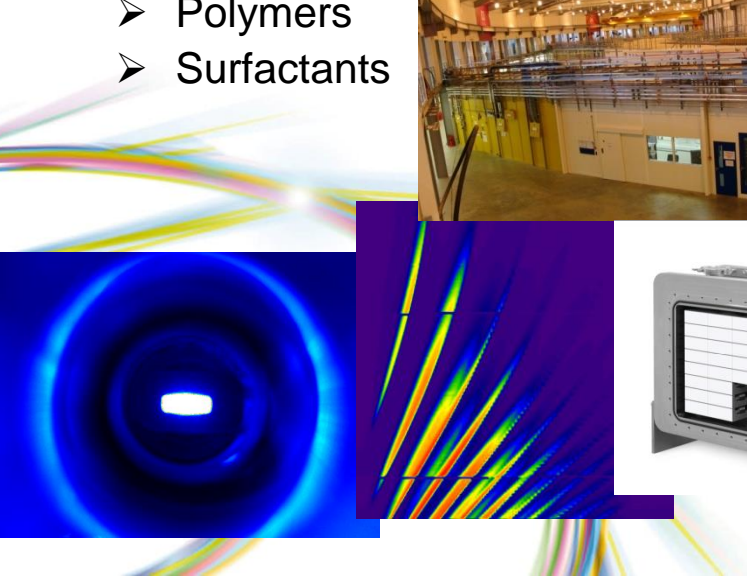
Small-angle, non-crystalline diffraction provides essential information on the structure and dynamics of large molecular assemblies in low ordered environments. These are characteristic of living organisms and many complex materials such as polymers and colloids.



# SAXS at Diamond

## Beamline Progress and Science highlights

- Used for
  - Archaeology
  - Biology
  - Biomaterials
  - Ceramics
  - Colloids
  - Cultural heritage
  - Environmental science
  - Forensic science
  - Liquid crystals
  - Mineralised tissue
  - Polymers
  - Surfactants

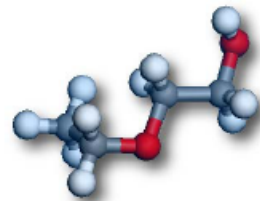


# Probing the Length Scales

Crystallography

Microstructure

Structure



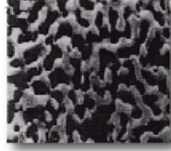
Atomic Structures



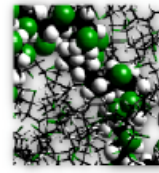
Proteins



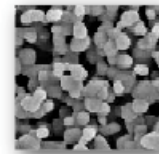
Micelles



Porous Media



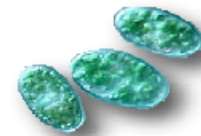
Polymers



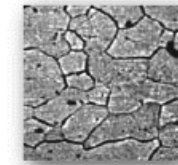
Precipitates



Viruses



Bacteria



Grain Structures

DIFFRACTION

X-ray, n, e

SANS/SAXS

10-1000 Å

TEM

USANS/USAWS

Optical microscopy

Light scattering

$10^{-11} \text{ m}$

$10^{-9}$

$10^{-7}$

$10^{-5}$

$10^{-3}$

10<sup>-11</sup> m

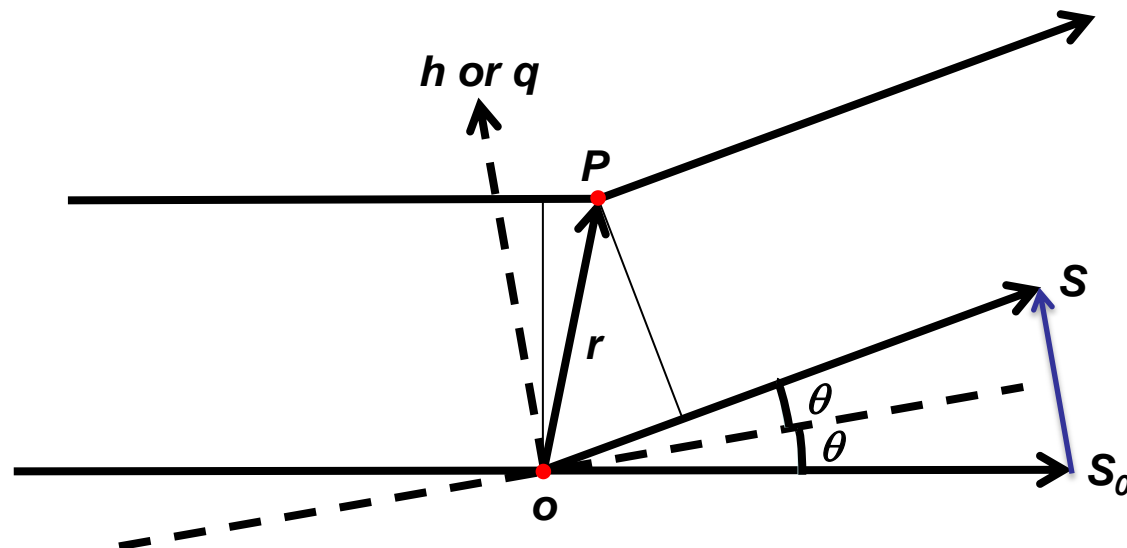


# Scattering

X-ray scattering is probing distances that are large compared to inter-atomic distances. Characteristics are:

- Random orientation of particles (i.e. no long-range order) leads to scattering rather than diffraction (determination of size and shape)
- Electron density variations at the particle-matrix interface cause x-rays to scatter.
- The scattered intensity,  $I(q)$ , is measured in terms of the scattering vector,  $q$ .

# Scattering by two point centres



From G. Porod, Ch2 in “Glatter and Kratky”

# X-ray scattering

Amplitude:  $A(q) = \int_{Vr} \rho(r) e^{-ir \cdot q} dVr$  (Volume Integral)

Where  $\rho(r)$  is the relates to the electron density  
and  $q$  is the scattering angle

Particle in solution => thermal motion => Particles have a random orientation/x-ray beam. The sample is **isotropic**. Only the **spherical average** of the scattered intensity is experimentally accessible.

Intensity:  $I(q) = \langle A(q) \cdot A^*(q) \rangle$

# Porod's law: specific surface and interface

- When two media are separated by a sharp interface, the scattered intensity follows an asymptotic law in the high  $q$  region:

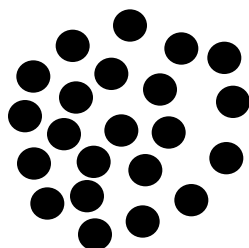
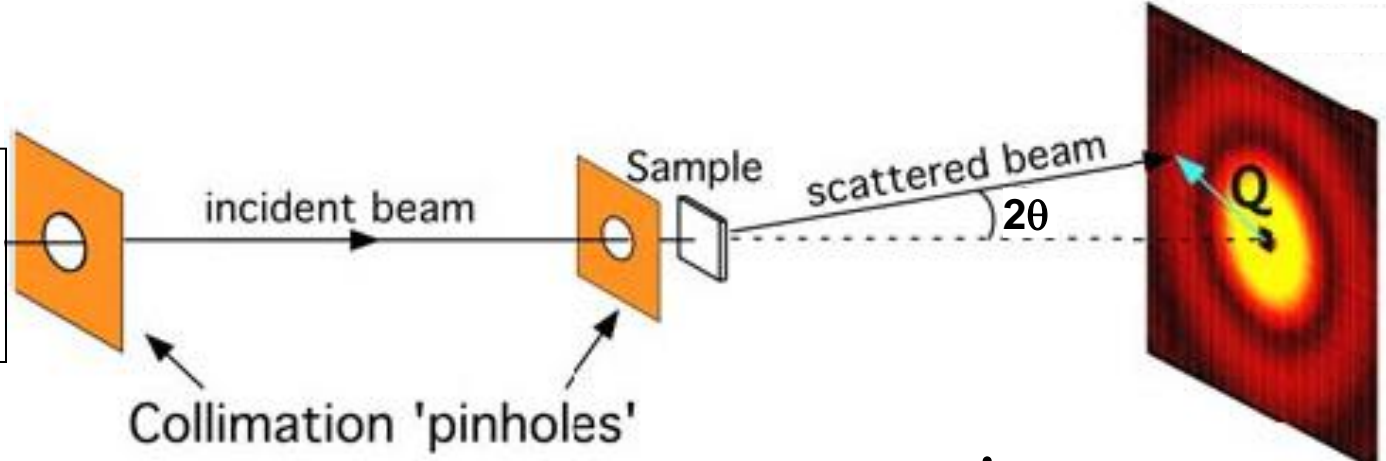
$$I(q) = Aq^{-4} + B.$$

- This law is called the Porod's limit and has more sophisticated expressions in the case of complicated interfaces.
- The asymptotic value, when the electronic contrast of the sample is known, and when the intensity is expressed in absolute scale, allows the calculation of the specific surface  $S$  (in  $\text{cm}^2/\text{cm}^3$ ) of the particles.

# Surface Fractal Laws

- For a smooth surface  $S(r) = r^2$ , and for a rough surface  $S(r) = r^{ds}$ , where  $ds$  is the surface fractal dimension that varies from 2 to 3
  - $I(q)$  proportional to  $q^{ds-6}$
- Surface fractals display power-law decays weaker than Porod's Law and are termed positive deviations from Porod's Law.

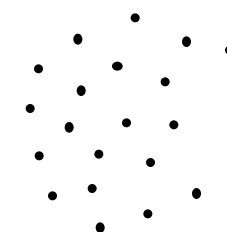
Source.  
Monochromator,  
Optics



Solution  
 $I(c,q)$

$$= \bullet * \bullet .$$

Motif (Protein)  
 $P(0,q)$



Lattice  
 $S(c,q)$

$$I(q) \propto \frac{d \sum(q)}{d\Omega} = \frac{N}{V} V_{particle}^2 (\rho_{sample} - \rho_{matrix})^2 P(q) S(q)$$

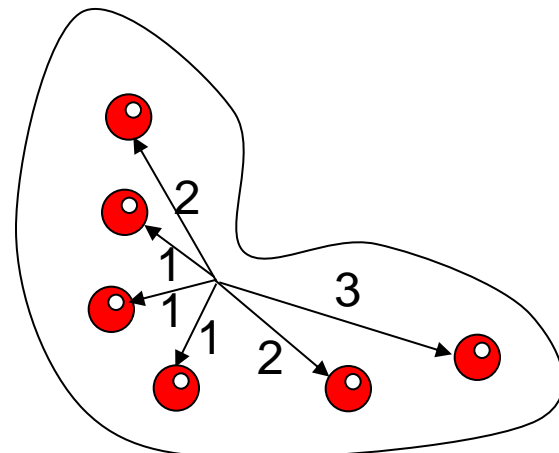
- $2\theta$  = scattering angle,  $\lambda$  = radiation wavelength
- $N$  = no. of scatterers in volume  $V$  of sample.
- $V_{particle}$  = volume of the individual scattering entity.
- $\rho$  = density of the particle or the matrix
- $P(q)$  = Form factor and  $S(q)$  = Structure Factor

- **From SAXS pattern:**
  - Particle size
  - Particle shape
  - Polydispersity
  - Kinetics

# What do we mean by “size”?

Radius of gyration:

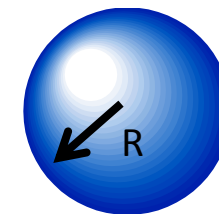
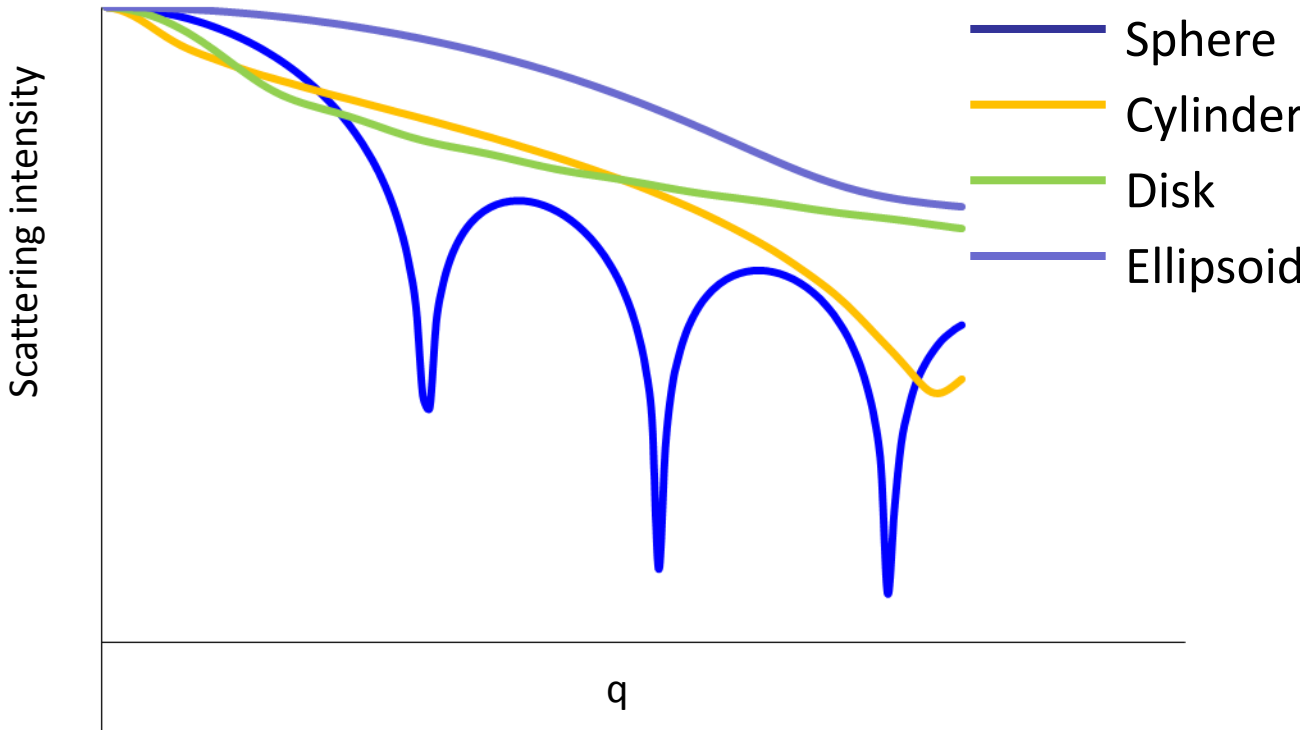
$R_g^2$  is the average squared distance of the scatterers from the centre of the object



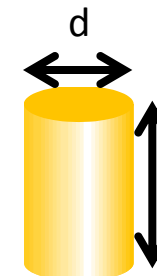
$$R_g^2 = (1^2 + 1^2 + 1^2 + 2^2 + 2^2 + 3^2)/6 = 20/6$$

$$R_g = \sqrt{3.333} = 1.82$$

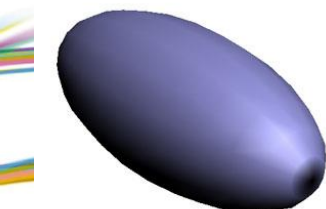
# Form Factor for simple shapes



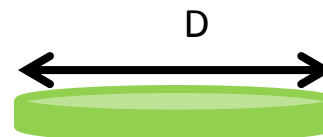
$$R_g = \sqrt{\frac{3}{5}} R$$



$$R_g = \frac{L}{\sqrt{12}}$$



$$R_g = \sqrt{\frac{1}{3} \left[ \left( \frac{a}{b} \right)^{\frac{4}{3}} + 2 \left( \frac{b}{a} \right)^{\frac{2}{3}} \right]}$$



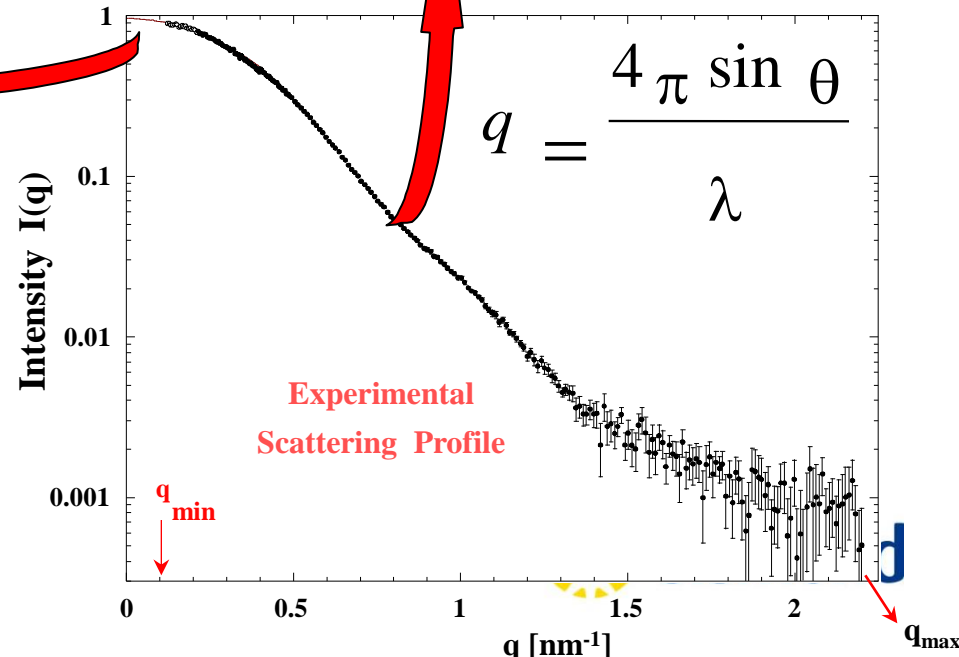
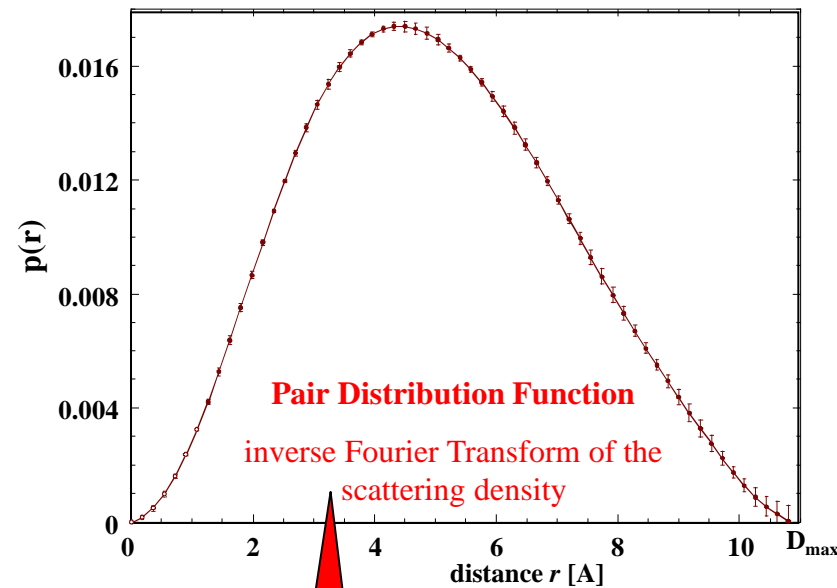
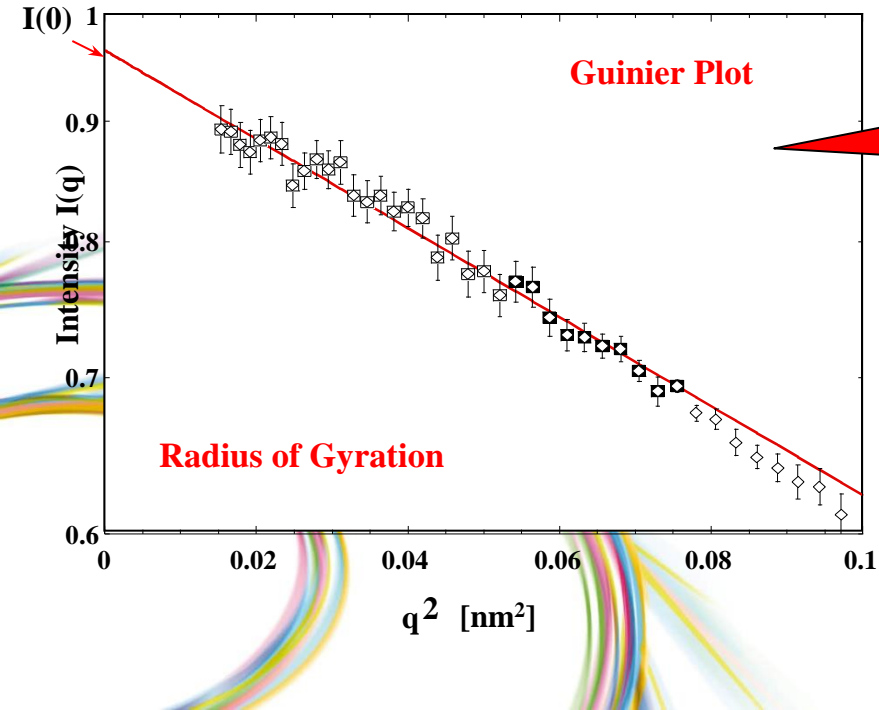
$$R_g = \frac{D}{2\sqrt{2}}$$

For more complicated shapes see reviews by J. S. Pedersen –  
<http://www.chem.au.dk/~jansp/resdescription.html>

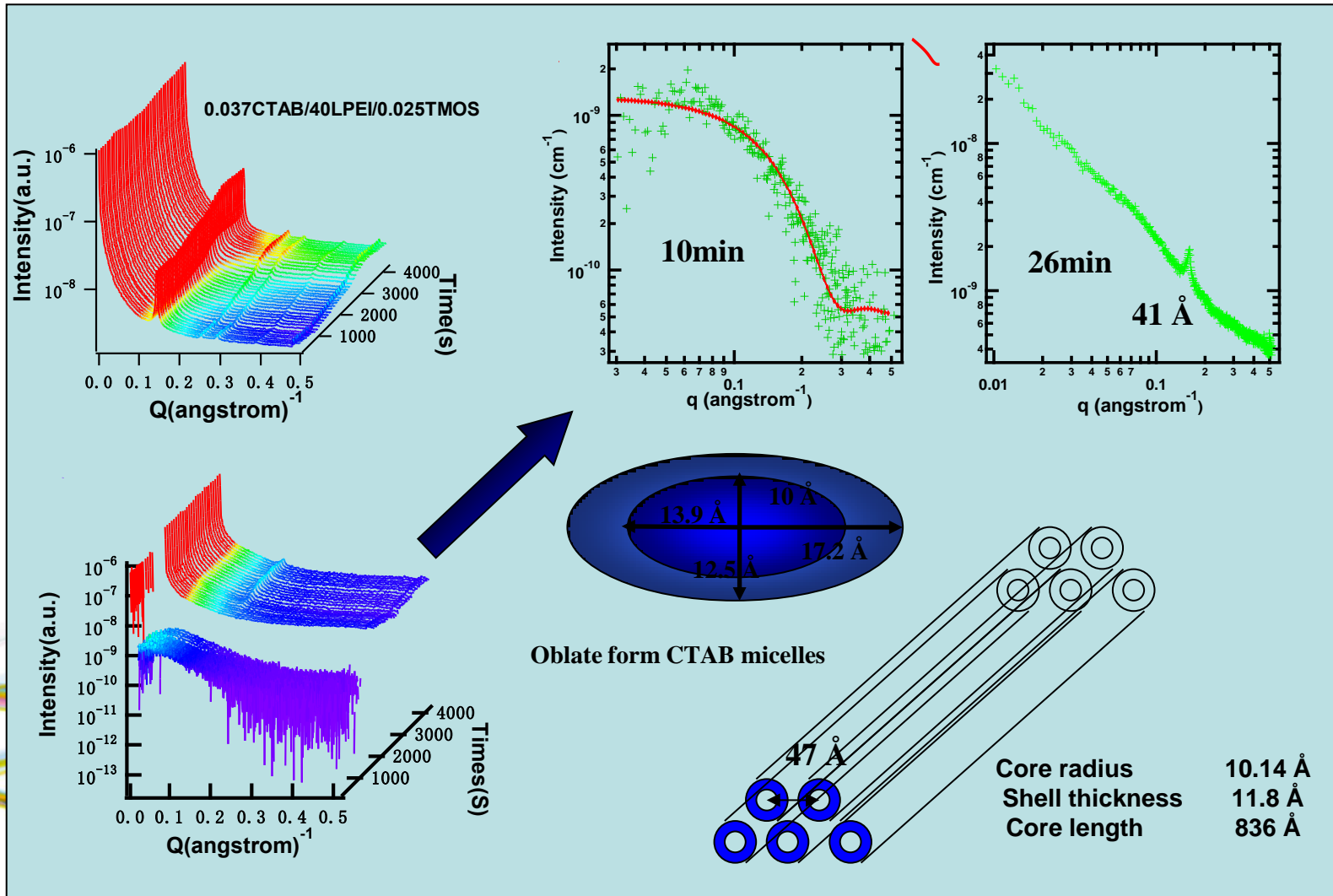
# Solution SAXS: $R_g$ , $I_0$ and $P(r)$

**Rg** = slope = shape function  
independent radius  
**I (at q=0)** or intercept  
proportional to number of  
particles / volume of solution

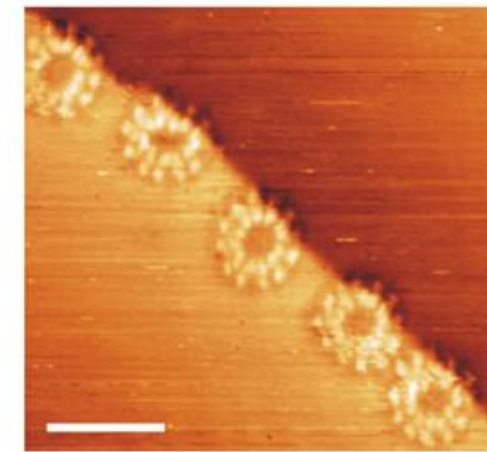
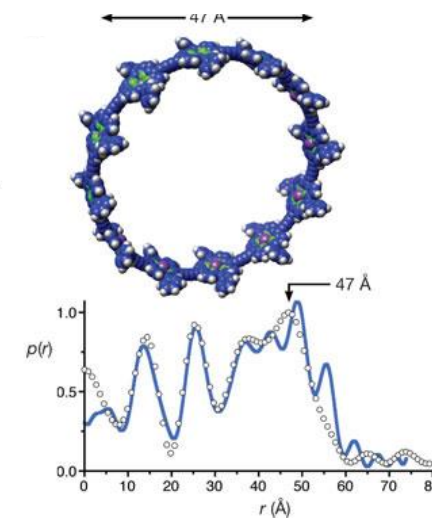
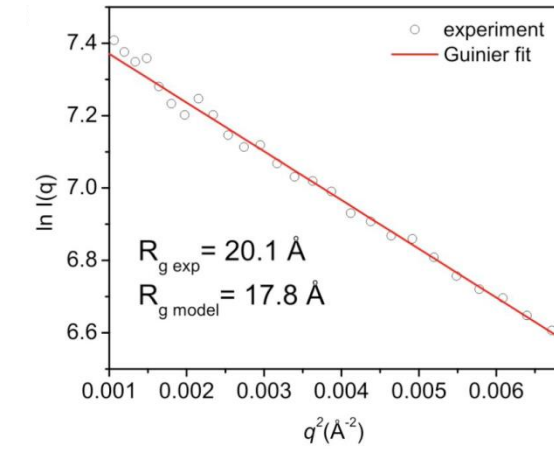
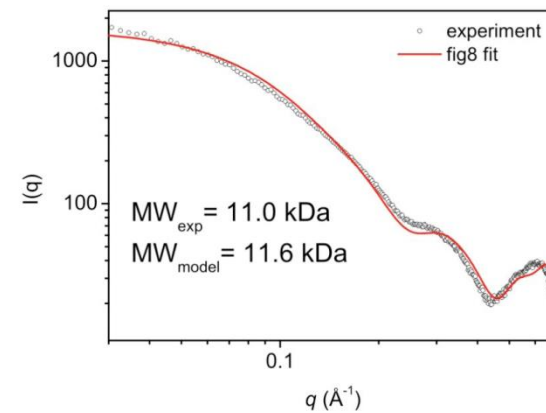
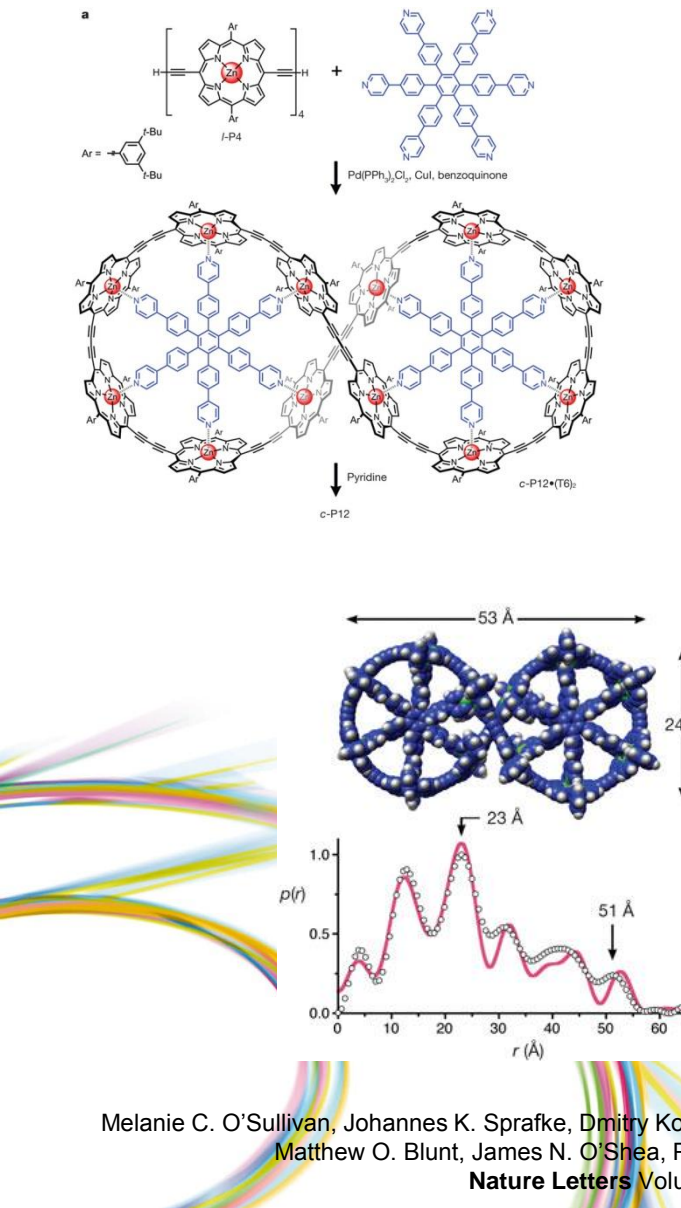
**PDF** = shape and size info



# SAXS studies on silica templated with polyelectrolyte-surfactant complexes



# Vernier templating and synthesis of a 12-porphyrin nanoring.



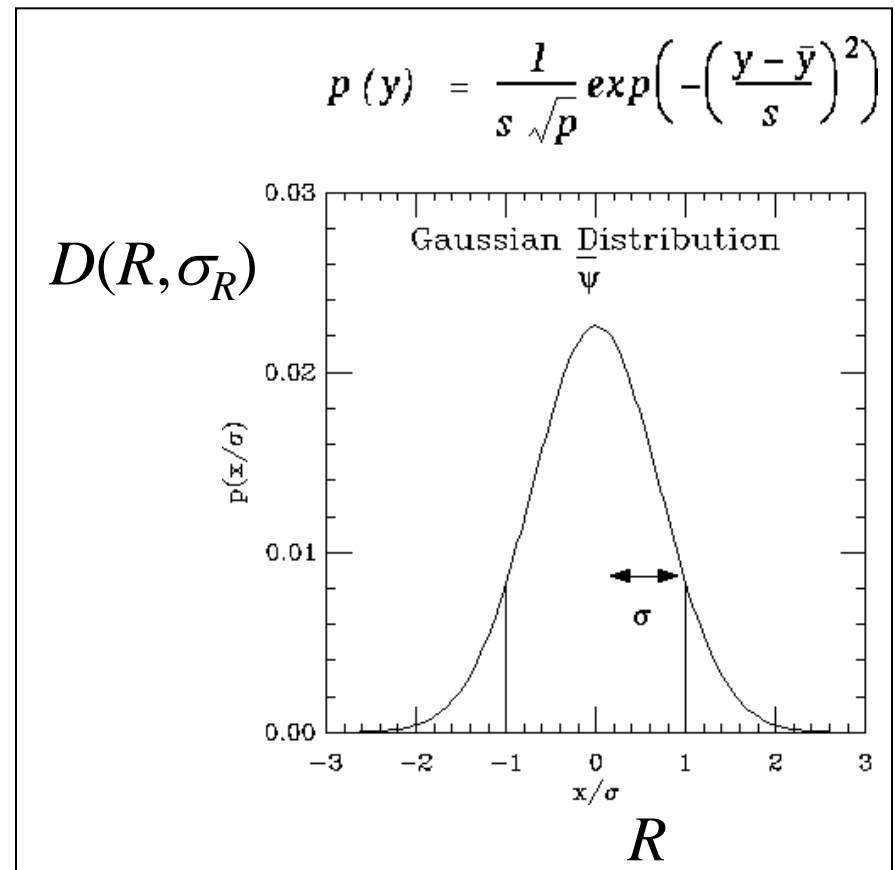
Melanie C. O'Sullivan, Johannes K. Sprafke, Dmitry Kondratuk, Corentin Rinfray, Timothy D. W. Claridge, Alex Saywell, Matthew O. Blunt, James N. O'Shea, Peter H. Beton, Marc Malfois, Harry L. Anderson,  
**Nature Letters** Volume: 469, Pages: 72–75, 2011

# Size polydispersity

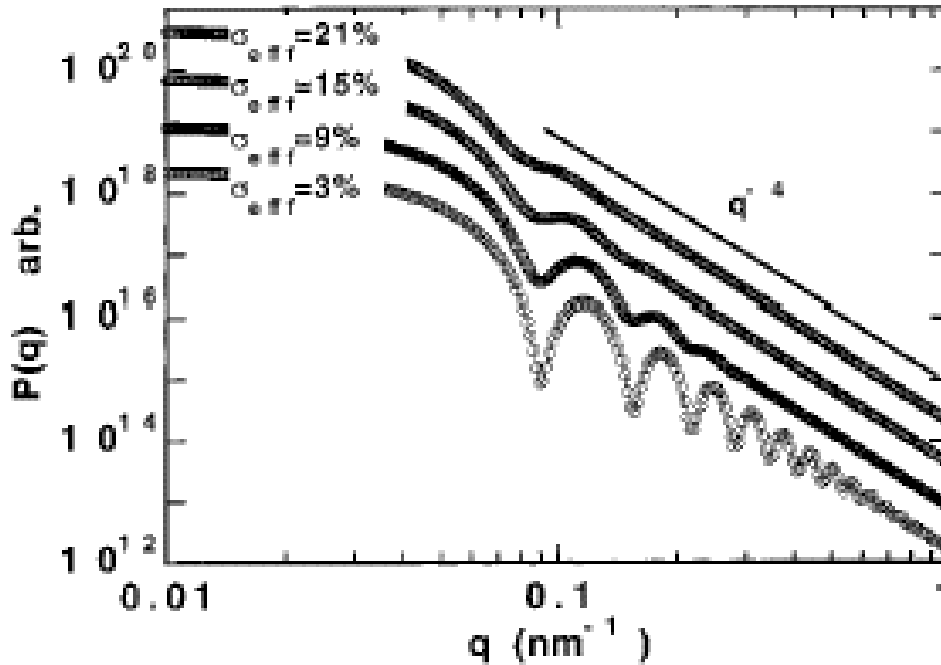
$$I(q) = \Delta\rho^2 \int_0^\infty P(q, R) D(R, \sigma_R) dR$$

$$P(q, R) = \left[ V \frac{3[\sin(qR) - qR \cos(qR)]}{(qR)^3} \right]^2$$

$$D(R, \sigma_R) = \frac{1}{\sigma_R \sqrt{2\pi}} \exp \left[ -\frac{(R - R_a)^2}{2\sigma_R^2} \right]$$



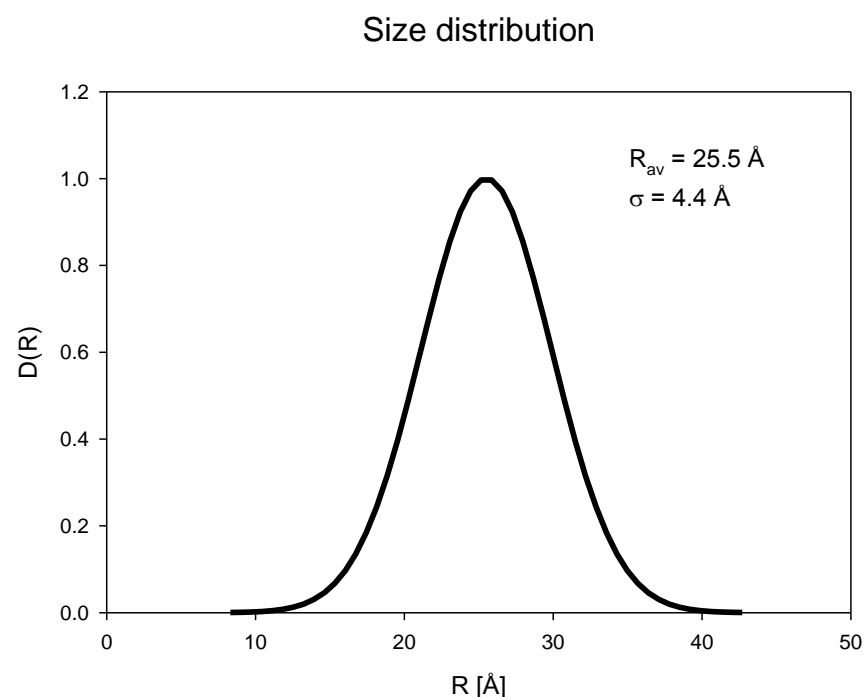
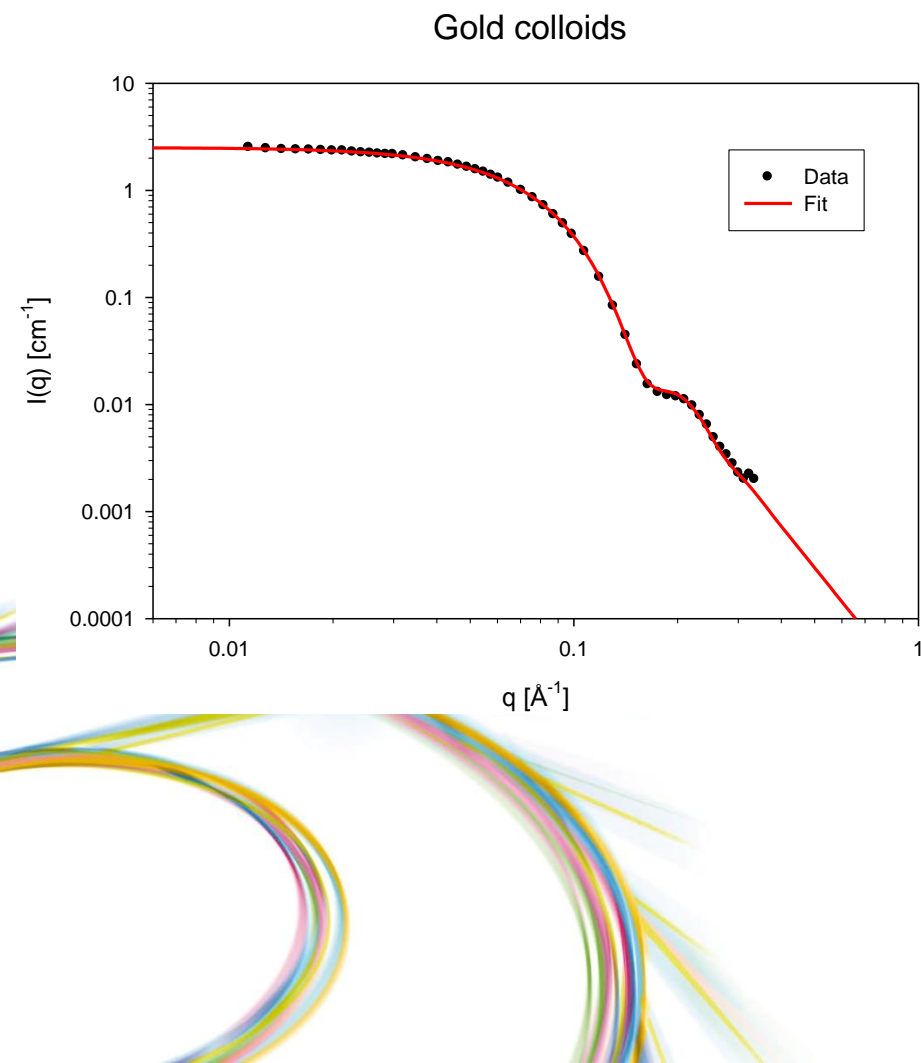
# Size polydispersity

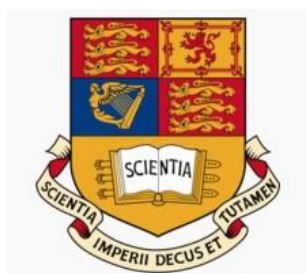


Smeared form factor  $P(q)$  for a sphere vs  $q$  showing the damping of Porod oscillation with increasing polydispersity ( $\sigma_{\text{eff}}$ ). The oscillations disappear for  $\sigma_{\text{eff}} > \sim 0.21$ . The mean particle diameter  $a_0 = 100\text{nm}$  for all calculations. Note the overall  $q^{-4}$  power law for  $q > 0.01\text{nm}^{-1}$ . The calculations terminate in the Guinier regime at low  $q$ .

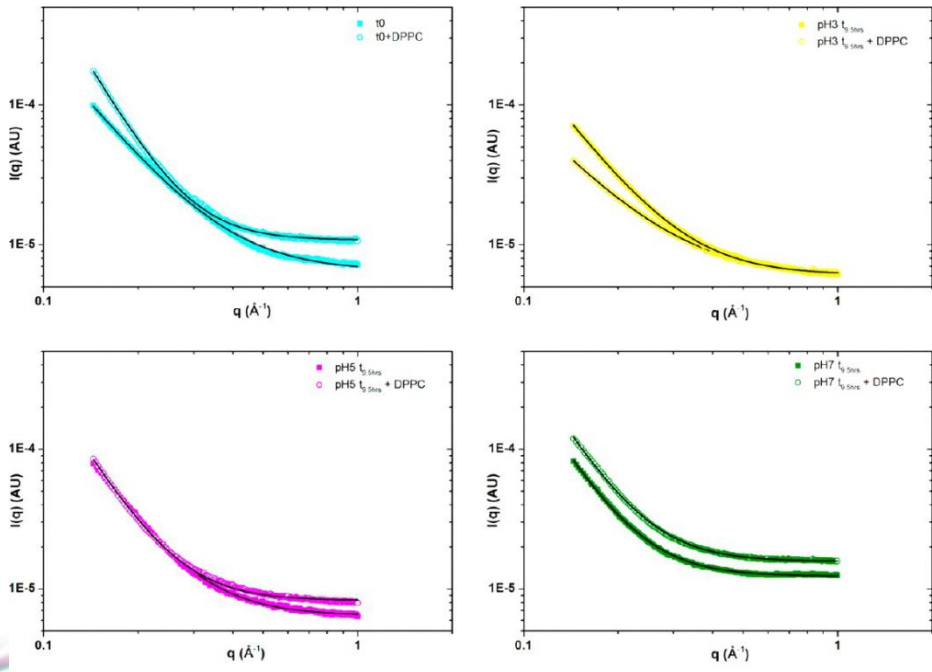
# Gold colloid

The spherical gold colloidal particles coated with thiols can be dissolved in an organic solvent like toluene

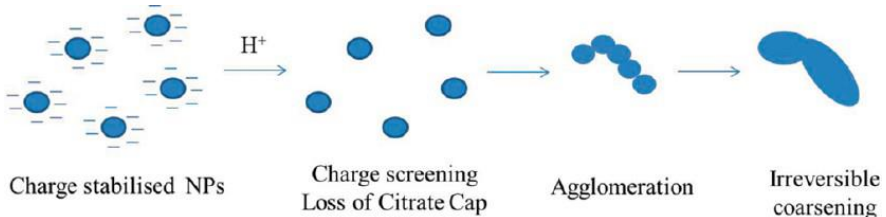
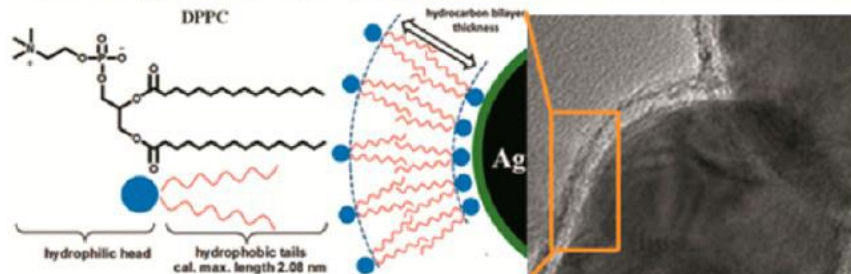
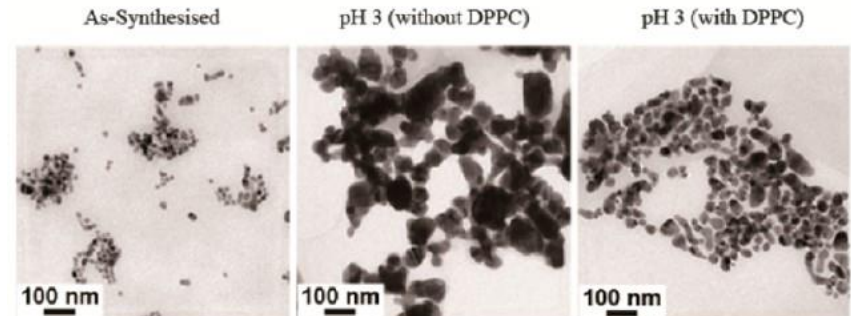




# The Stability of Silver Nanoparticles in a Model of Pulmonary Surfactant

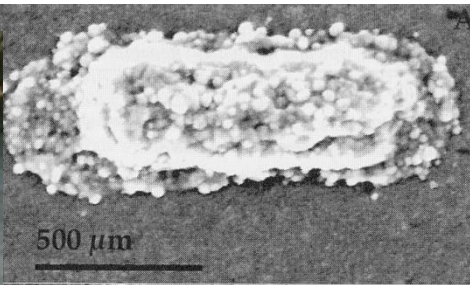


	As made, t=0 -DPPC	pH3, t=9.5 hrs -DPPC	pH3, t=9.5 hrs +DPPC	pH5, t=9.5 hrs -DPPC	pH5, t=9.5 hrs +DPPC	pH7, t=9.5 hrs -DPPC	pH7, t=9.5 hrs +DPPC	
R <sub>s</sub> (nm)	7.1	7.0	21.3	10.9	15.1	10.4	7.7	7.0
D (nm)	18.6	18.0	55.0	28.0	39.1	26.8	19.8	18.8
χ² (x 10⁻¹³)	1.2	2.3	0.5	0.5	1.0	1.3	0.6	1.6



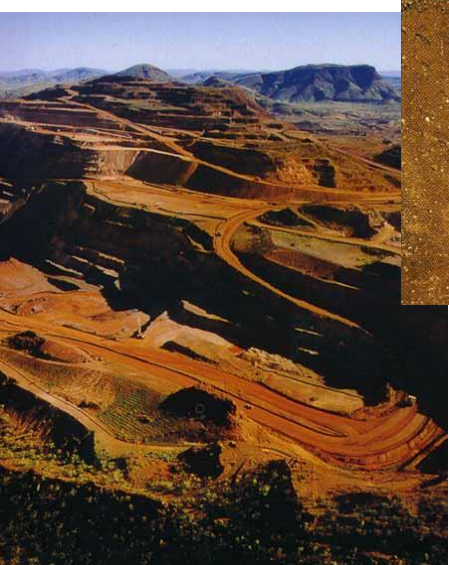
Bey Fen Leo, Shu Chen, Yoshihiko Kyo, Karla-Luise Herpoldt, Nicholas J. Terrill, Iain E. Dunlop, David S. McPhail, Milo S. Shaffer, Stephan Schwander, Andrew Gow, Junfeng Zhang, Kian Fan Chung, Teresa D. Tetley, Alexandra E. Porter, and Mary P. Ryan, *Environ. Sci. Technol.* 2013, 47, 11232–11240, DOI: 10.1021/es403377p front of the Huns local

# Iron oxyhydroxides in the environment



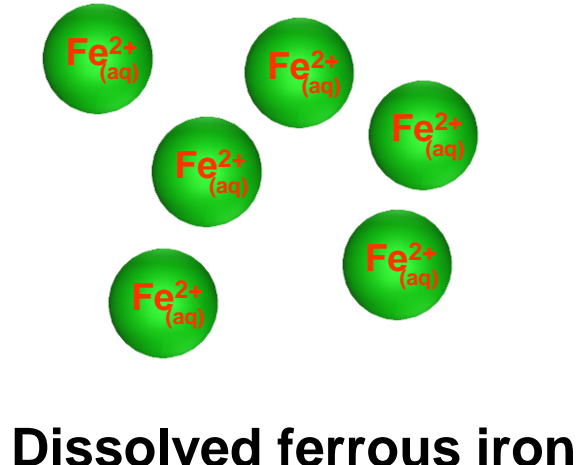
## Thermodynamics vs. Kinetics

- Most stable phases are goethite ( $\text{FeOOH}$ ) and hematite ( $\text{Fe}_2\text{O}_3$ )
- Poorly-ordered iron oxyhydroxide (ferrihydrite) very common in soils and sediments

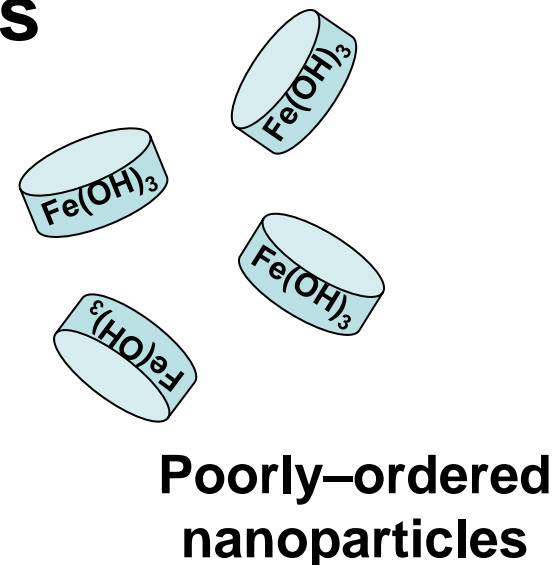


Iron oxyhydroxide  
bearing  
contaminant plume  
(Restronguet  
Creek, Cornwall)  
Acid mine  
drainage

# Formation of ferric oxyhydroxide nanoparticles

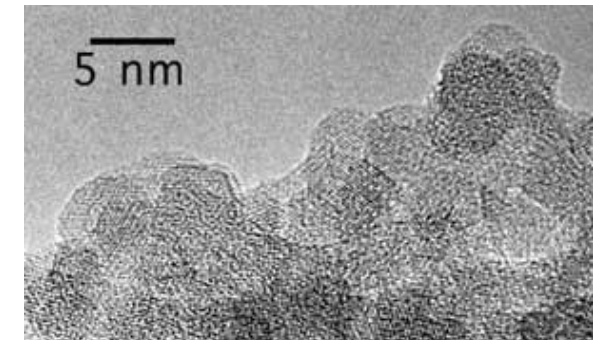
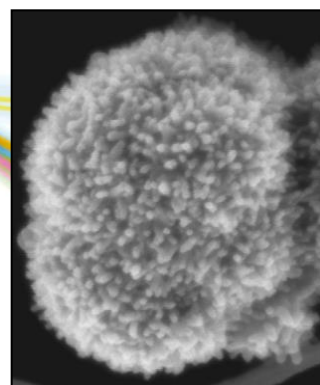


oxidation &  
hydrolysis



Schwertmannite  $\text{Fe}_{16}\text{O}_{16}(\text{OH})_{12}(\text{SO}_4)_2$

(Janney et al., 2000)



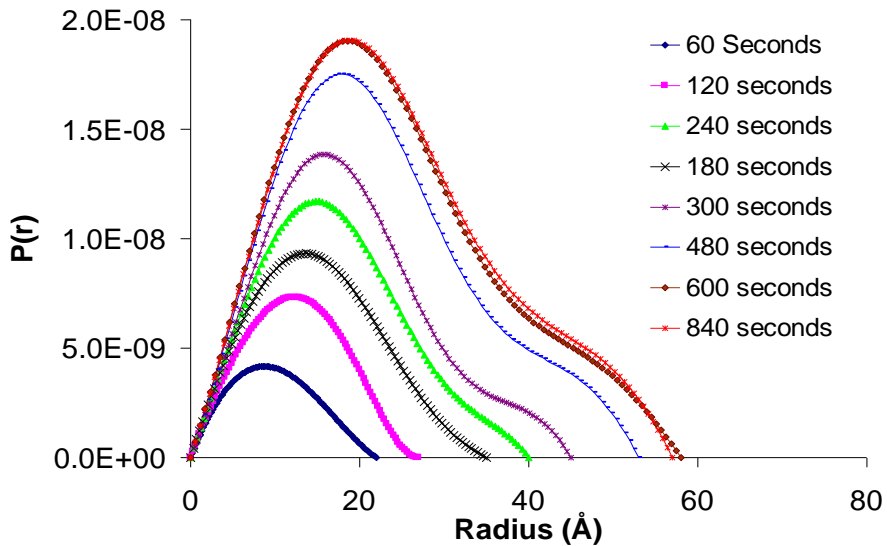
# Pair/Size distribution function (pure) (PDF/SDF)

pH = 4

## Pair distribution function

( $R_g$  more accurate: based on full scattering pattern not only low  $q$ )

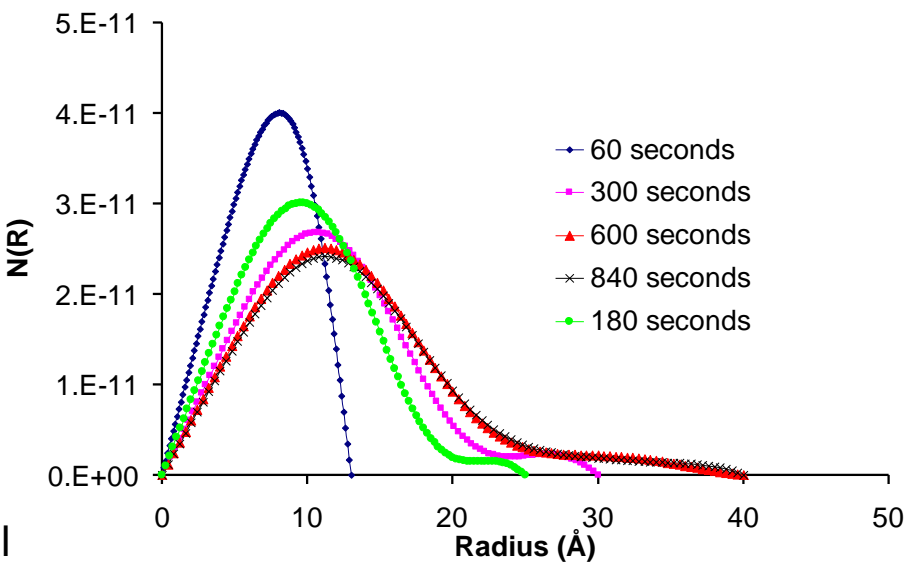
- Equant particle shape at beginning of reaction
- Elongated particles forming by end of reaction



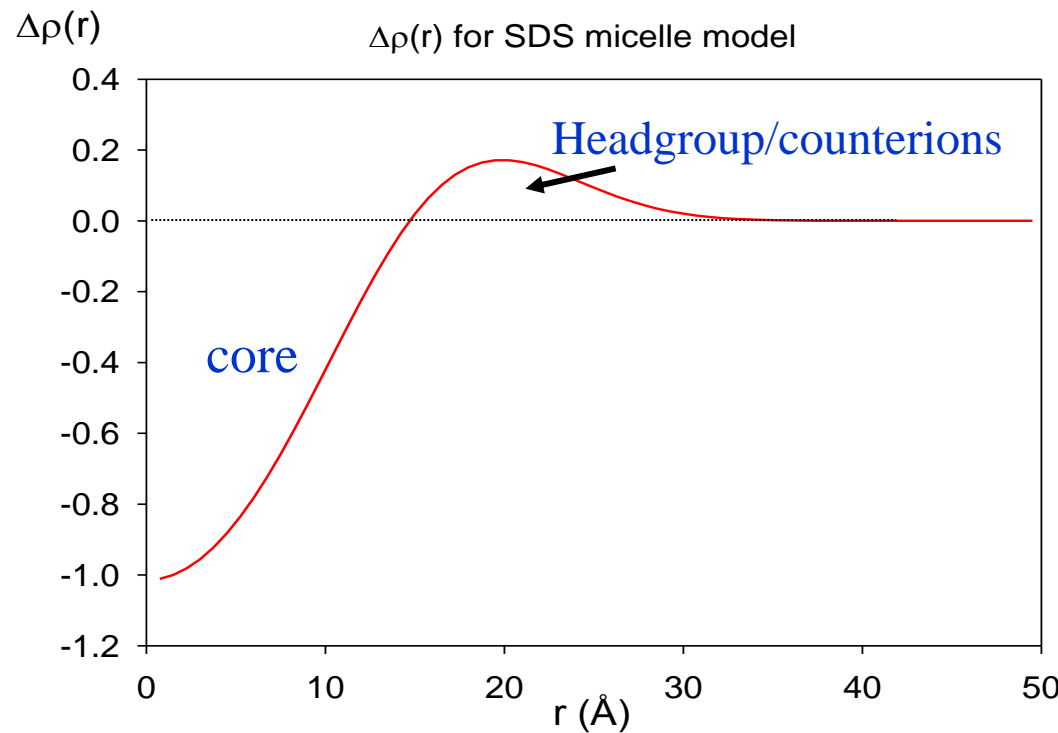
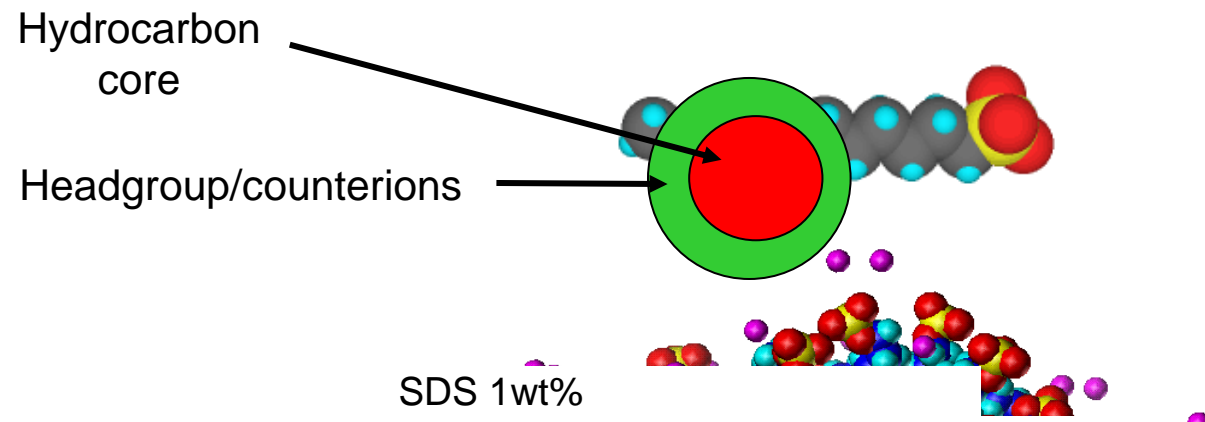
## Size distribution function

(degree of polydispersity)

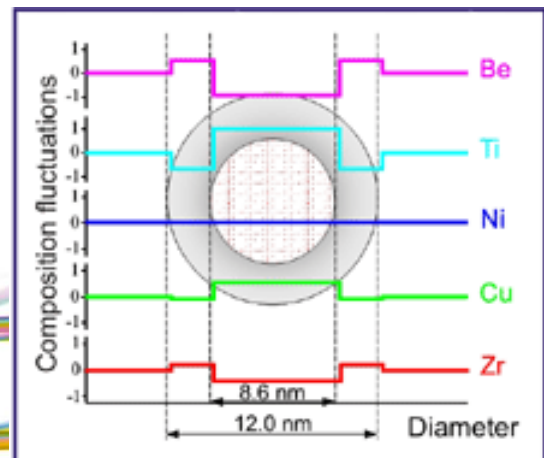
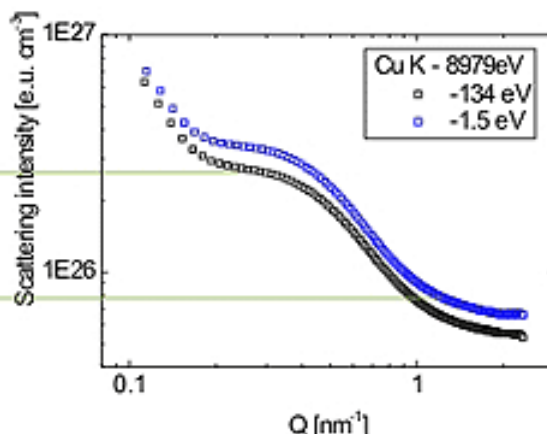
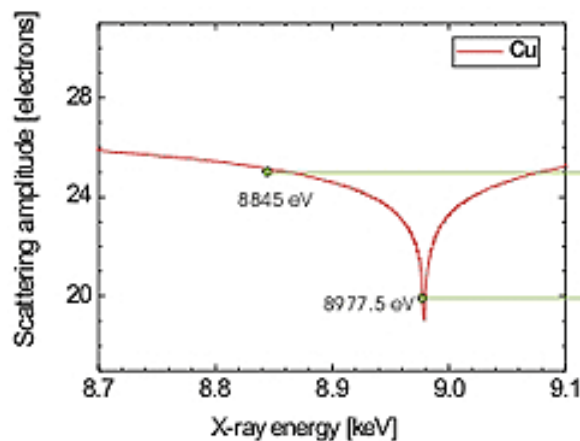
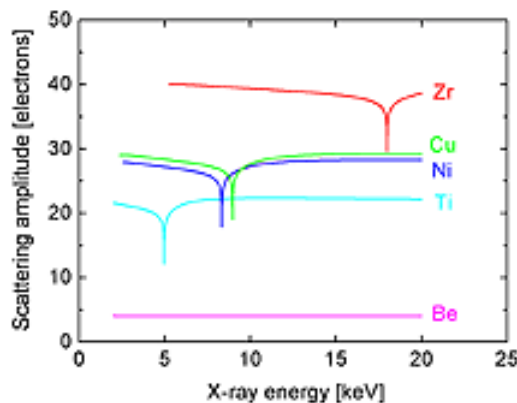
- Monodispersed system at beginning of reaction
- Slight increase in polydispersity with time



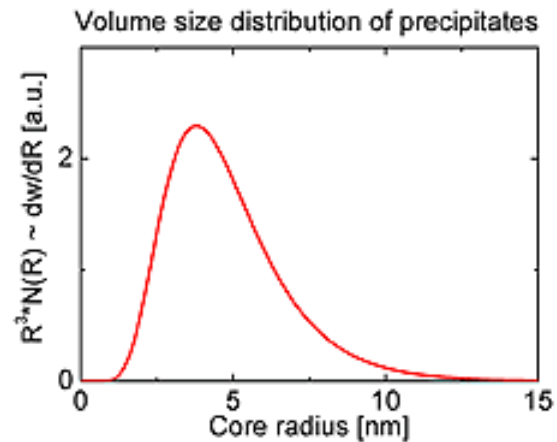
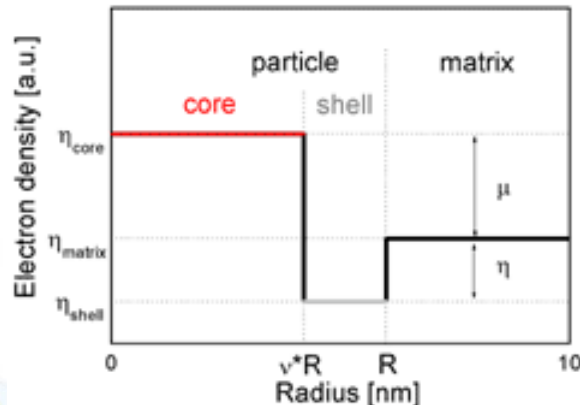
# SDS micelle (Soap!)



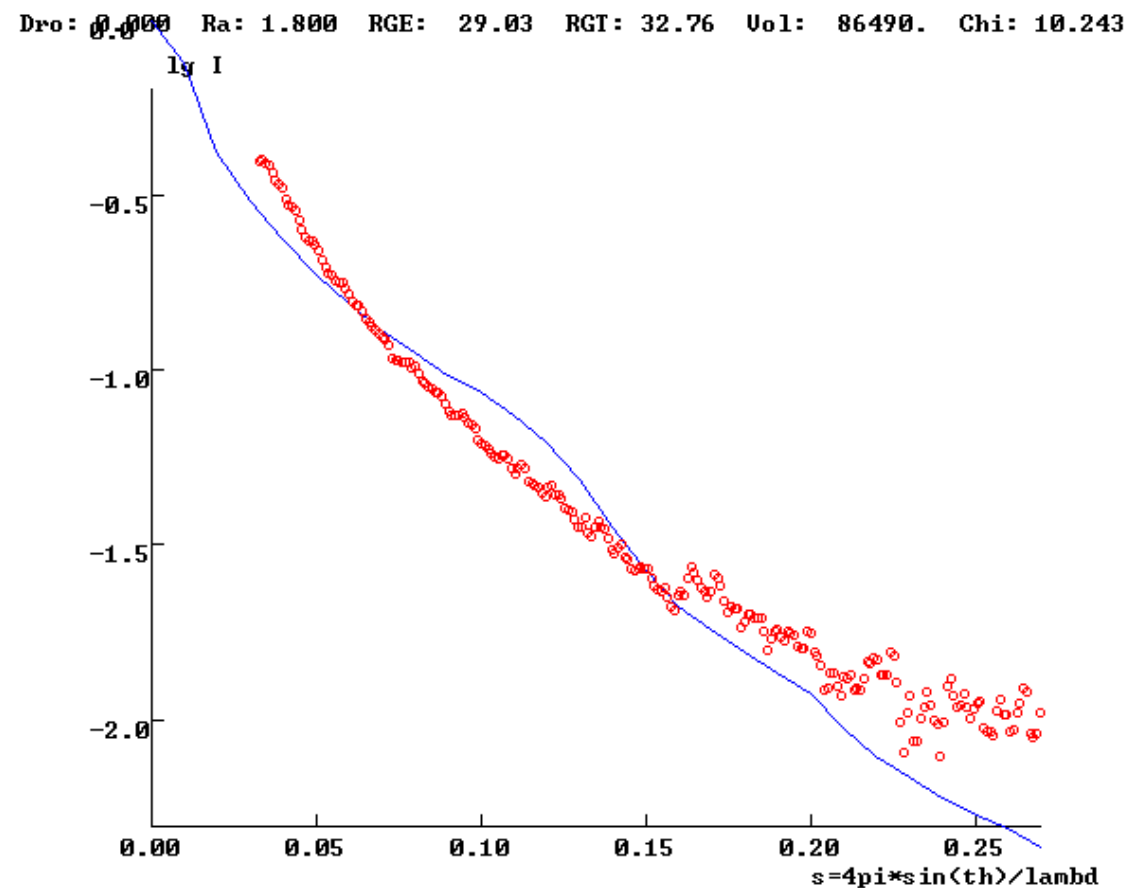
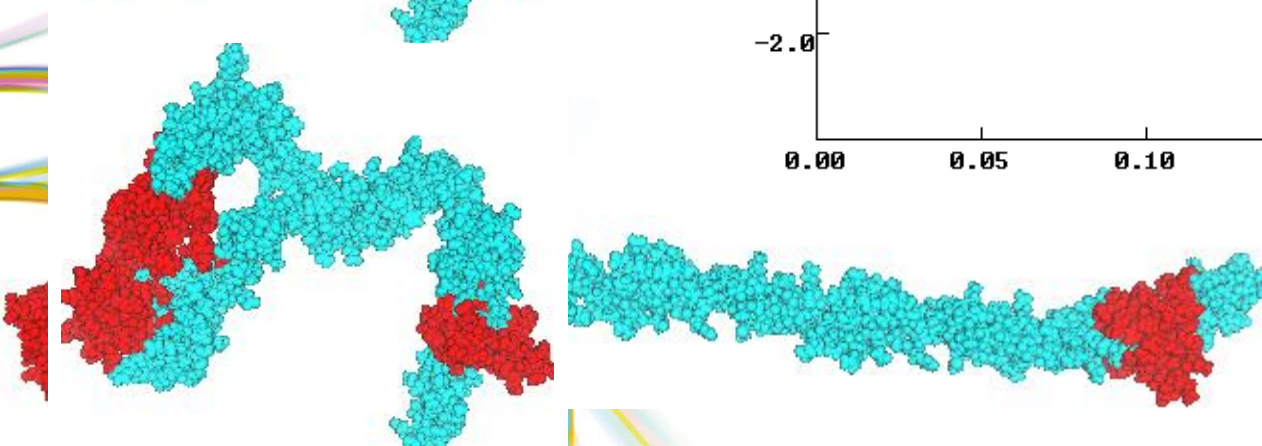
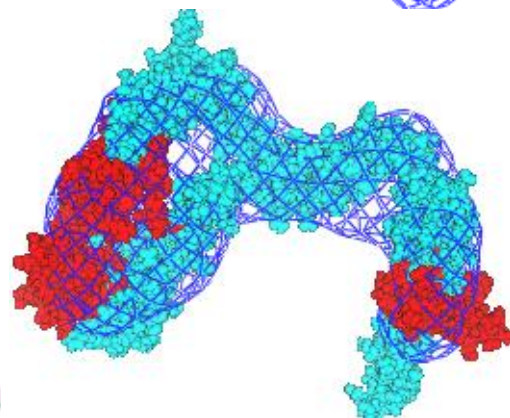
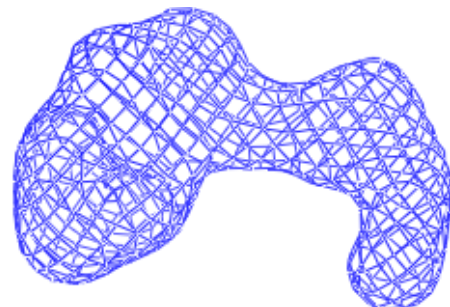
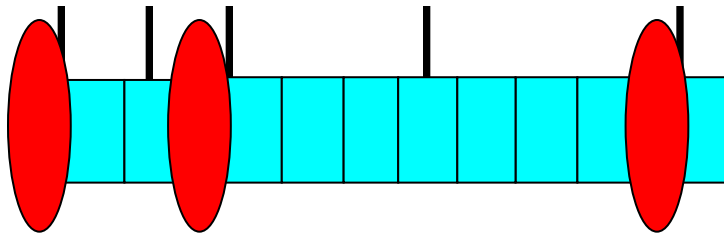
# ASAXS example from BESSY (Berlin)



Relative composition changes in the precipitation and surrounding depletion zone.

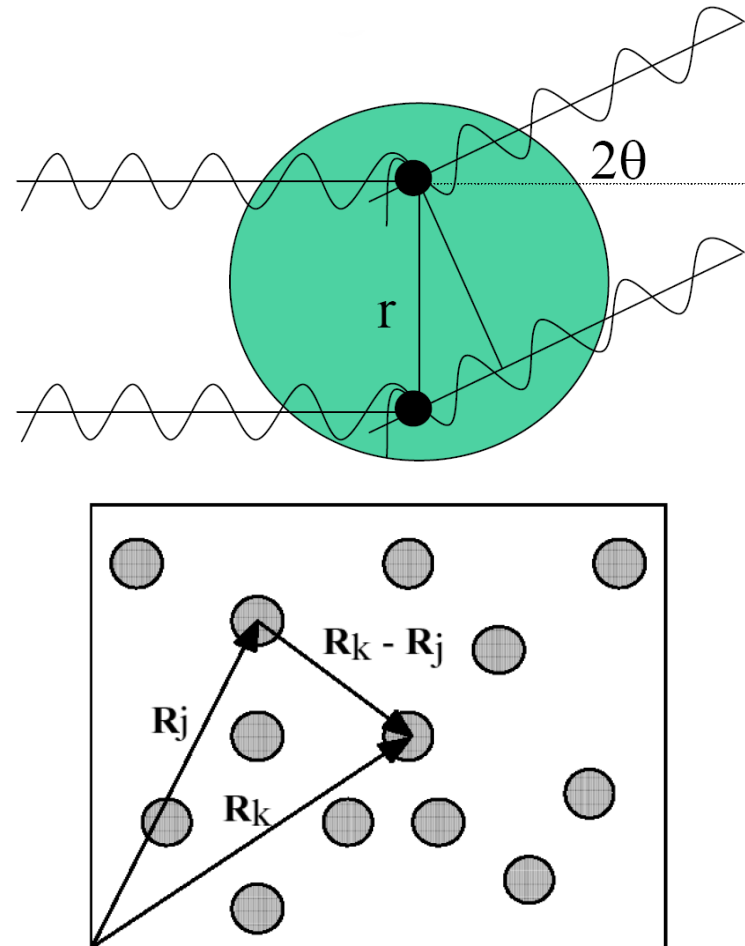


# Fibrillin Protein Fragment 13



# What if you have a Non-Dilute system?

- Scattering (Interference) determined by spatial dimensions
- Form Factor -  $P(q)$  - particle size and shape (intraparticle)
- **Structure Factor -  $S(q)$**  interparticle correlations function of local order and interaction potential; complex if correlation between position and orientation



# Concentration effects ( $S_q$ )

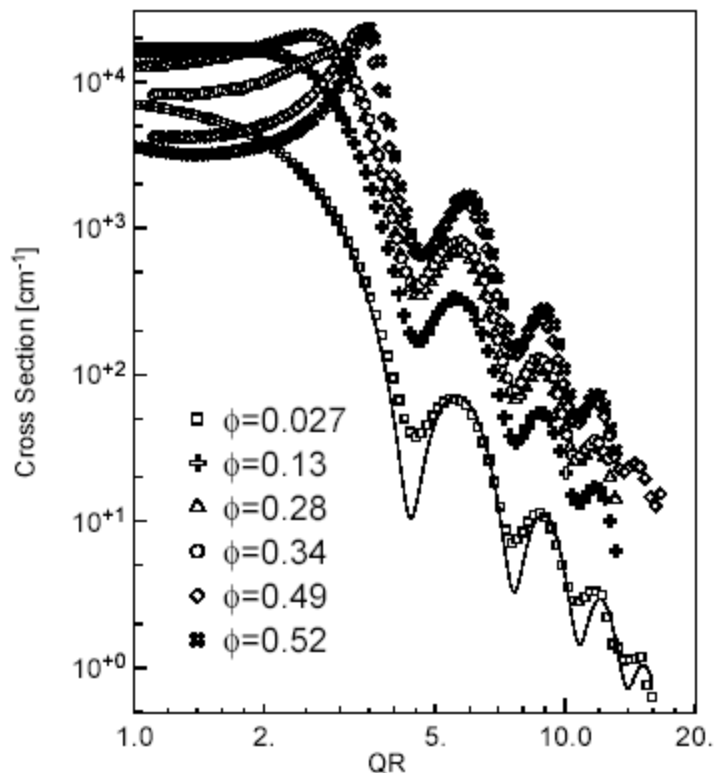


Figure 1: Cross-section for several different volume fractions of PS spheres in glycerol vs.  $QR$ .

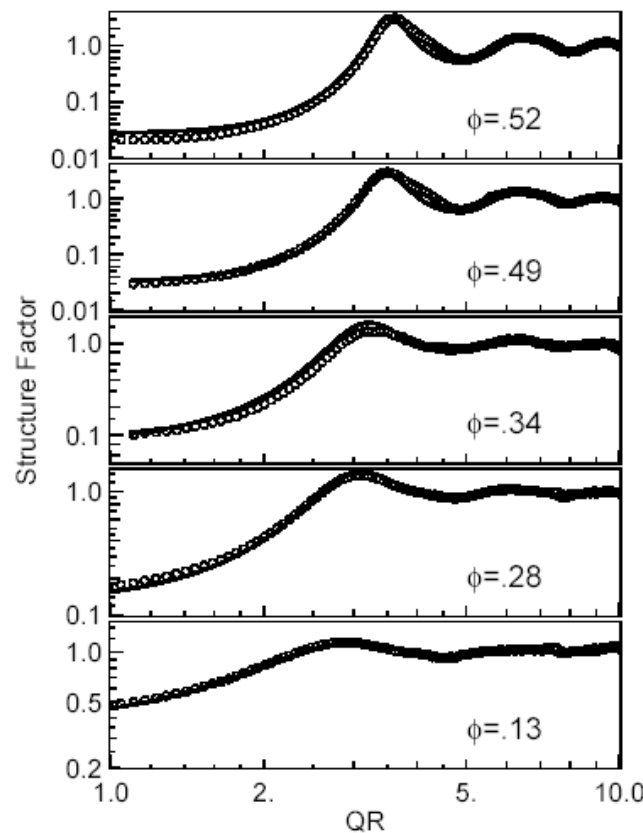


Figure 2: Measured and model structure factors,  $S(Q)$ , (circles and dashed lines, respectively) vs.  $QR$  for PS spheres in glycerol.

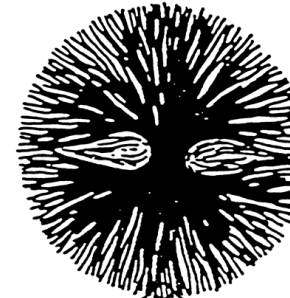
## Small Angle X-ray Scattering Study of a Hard-Sphere Suspension: Concentrated Polystyrene Latex Spheres in Glycerol

L. B. Lurio<sup>1</sup>, D. Lumma<sup>1</sup>, A. R. Sandy<sup>1</sup>, M. A. Borthwick<sup>1</sup>, P. Falus<sup>1</sup>, S. G. J. Mochrie<sup>1</sup>,  
J. F. Pelletier<sup>2</sup>, M. Sutton<sup>2</sup>, Lynne Regan<sup>3</sup>, A. Malik<sup>4</sup> and G. B. Stephenson<sup>4</sup>

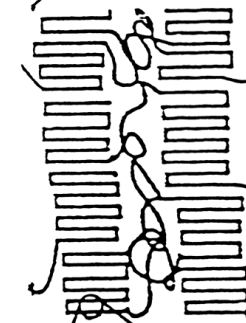


# Semicrystalline Block Copolymers

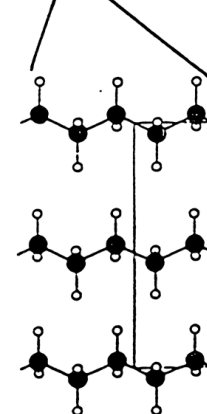
- Few commercial examples
- Crystallisable end blocks
- PE-PEP-PE (hPB-hPI-hPB)
- Low crystallinity PE look-alike
- Metallocenes for multi-blocks
- Very complicated phenomenology
- Break-out & confined crystallisation depending on morphology and  $T_g$  of noncrystallising material.



Spherulite  
 $O(10 \mu\text{m})$

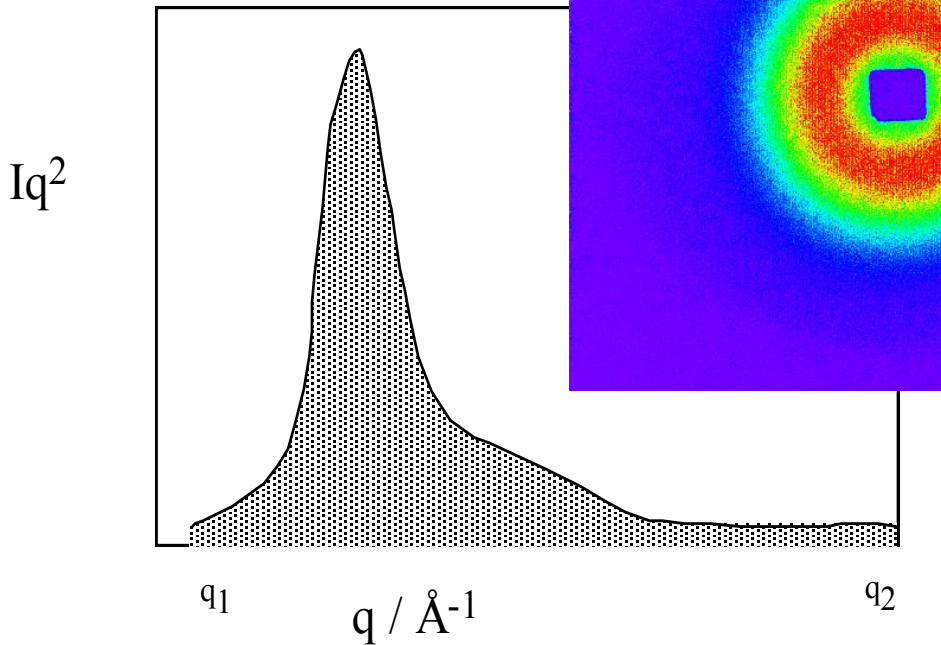


Lamella  
 $O(10-100 \text{ nm})$



Unit cell  
 $O(1-10 \text{ \AA})$

# Scattering at Small Angle



Bragg's law gives an estimate of interference function  $d=2\pi/q^*$  but how do we get the degree crystallinity and hence L?

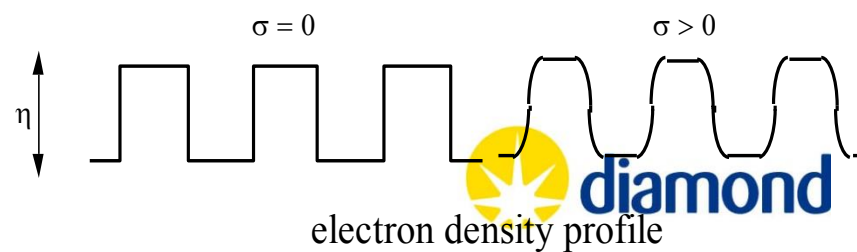
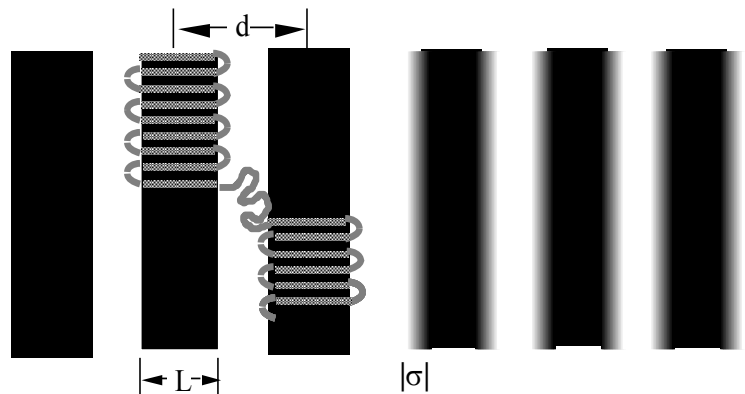
The scattering invariant

$$Q = \phi(1-\phi)\Delta\eta^2$$

$$Q = \int I(q)q^2 dq \text{ with limits } 0 \leq q \leq \infty$$

But the SAXS pattern has data in a range of  $q$

semicrystalline lamellar stacks



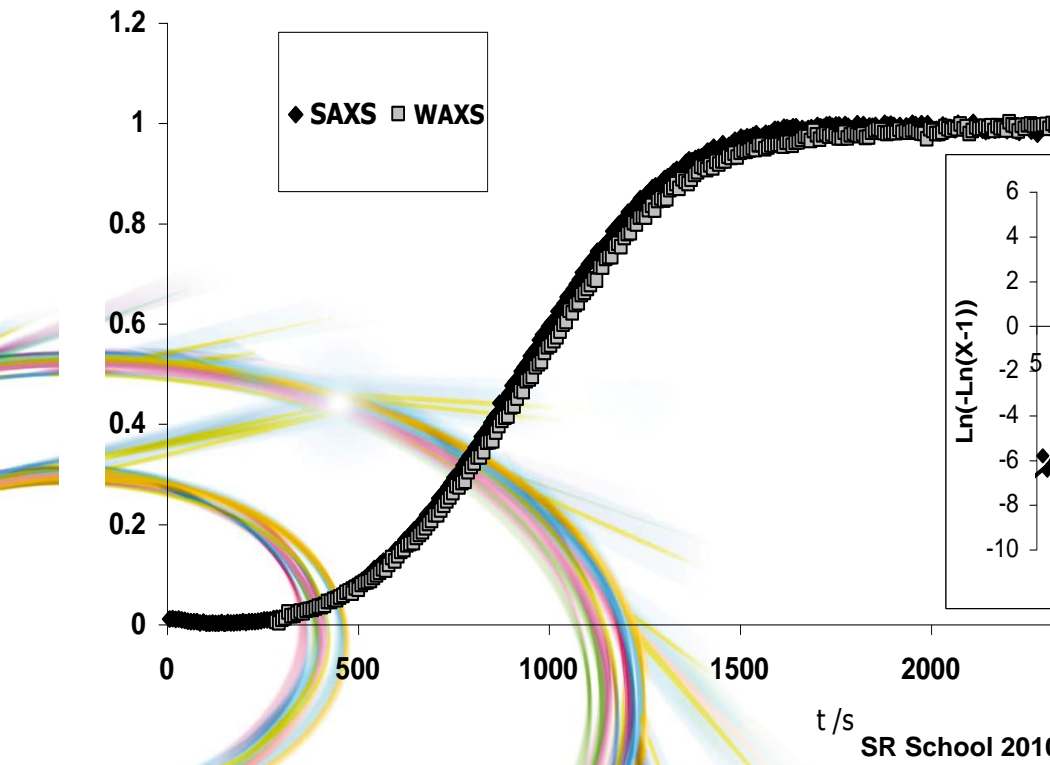
# SAXS Invariant

$$Q = \phi(1-\phi)\Delta\eta^2$$

$\phi$  and  $\Delta\eta$  in a lamellar stack  
do not change during crystallisation  
but the crystalline volume increases so

$$Q = X_s$$

*the volume fraction of spherulites*

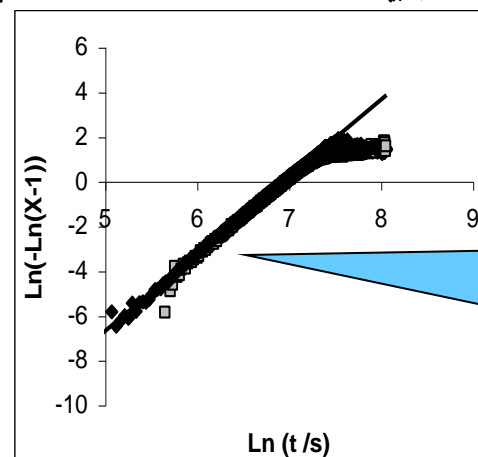


Kinetics from  
time-resolved  
(static) scattering

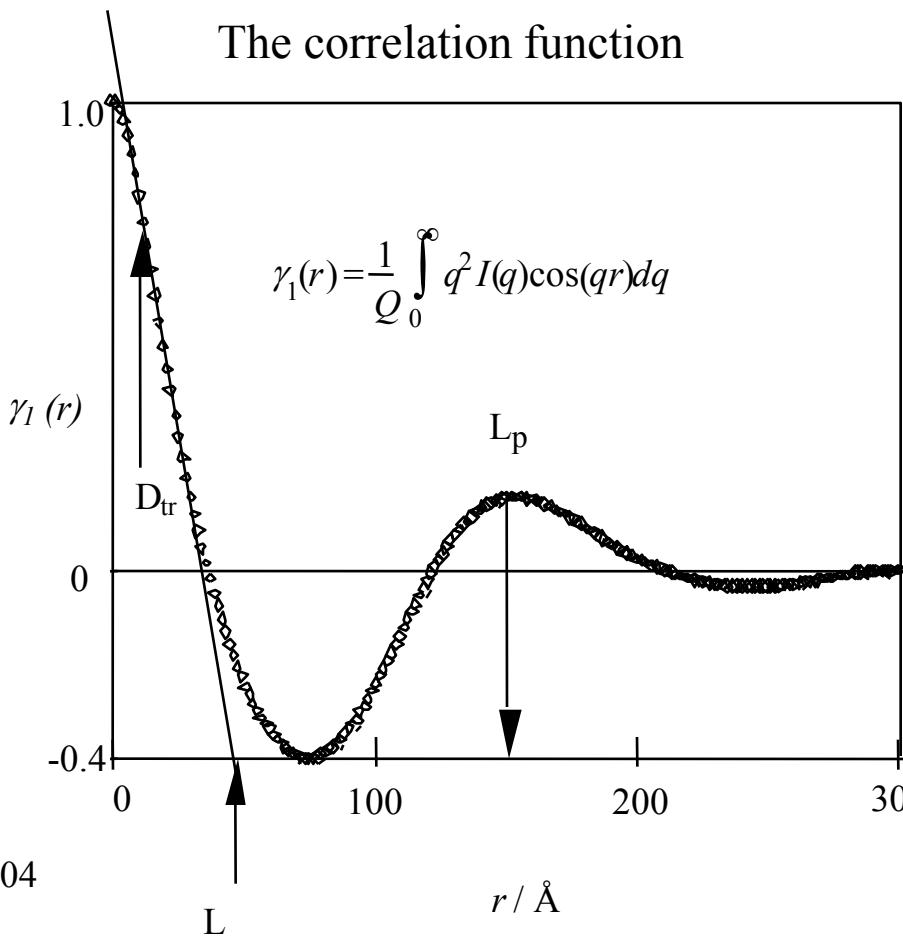
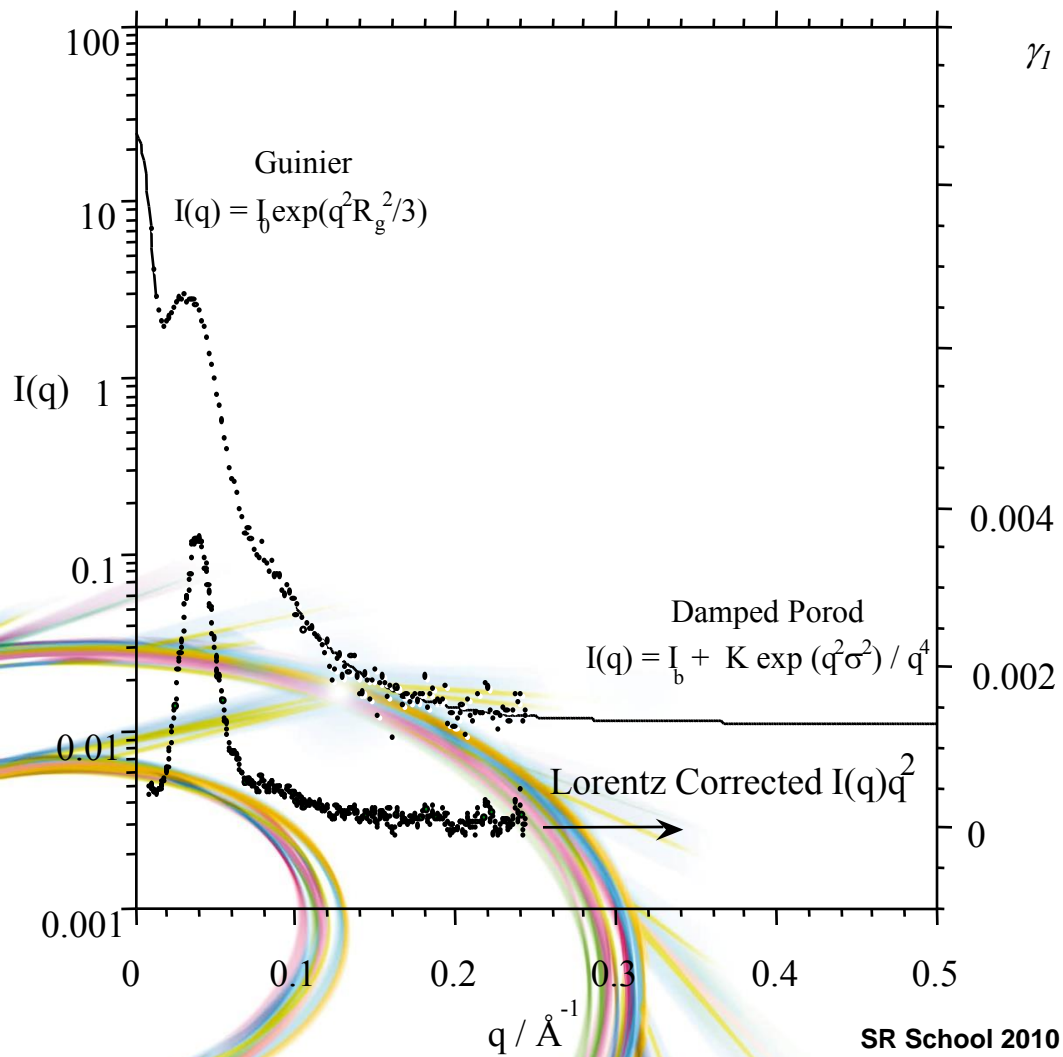
## WAXS

degree of crystallinity

$$X_c = A_c/(A_c + A_a)$$



# For Lamellae there is more!



## Correlation Function Analysis



# How does it work?



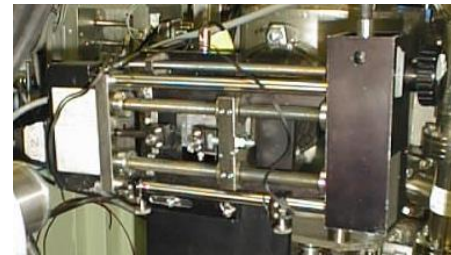
# Added Value from the sample



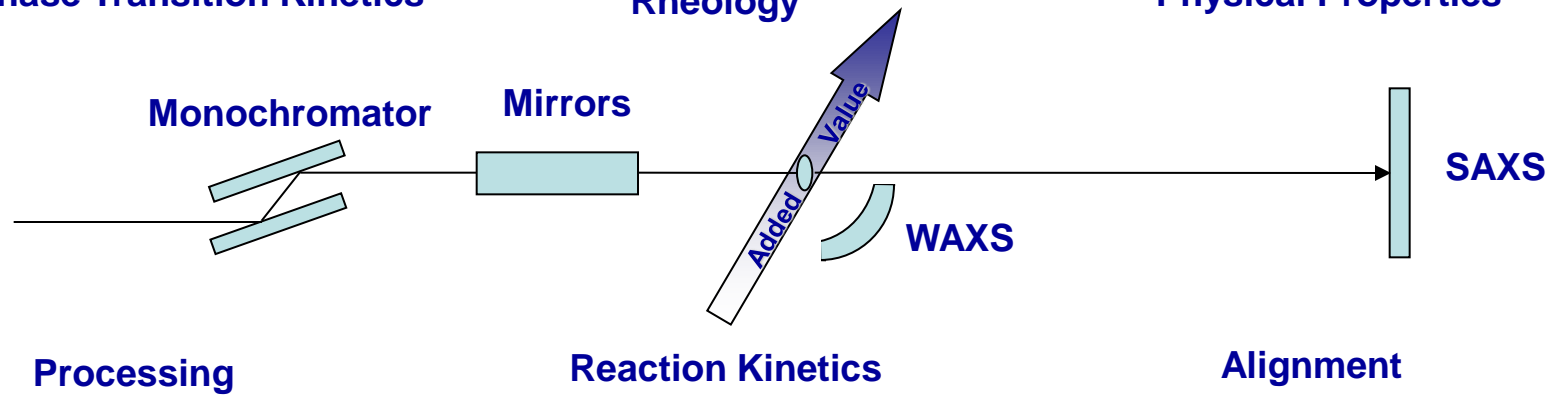
Phase Transition Kinetics



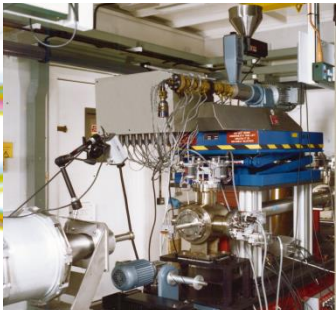
Rheology



Physical Properties



Processing



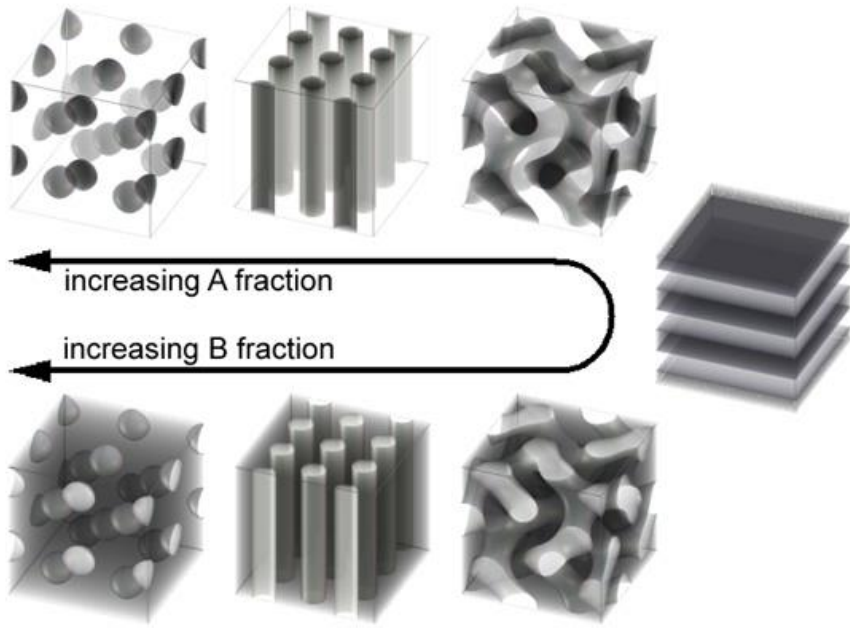
Reaction Kinetics



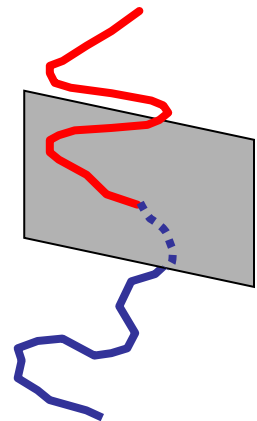
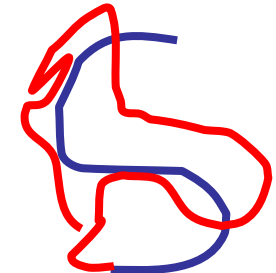
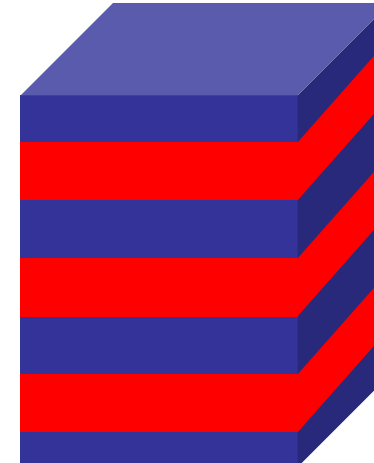
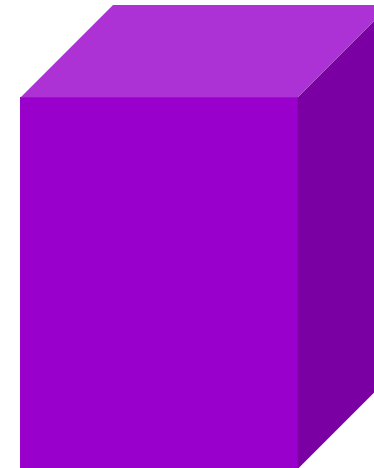
Alignment

# Block Copolymer Self Assembly

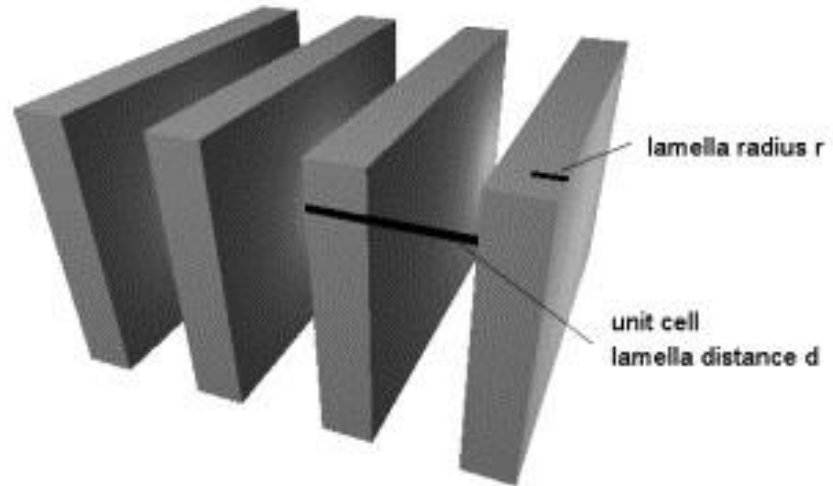
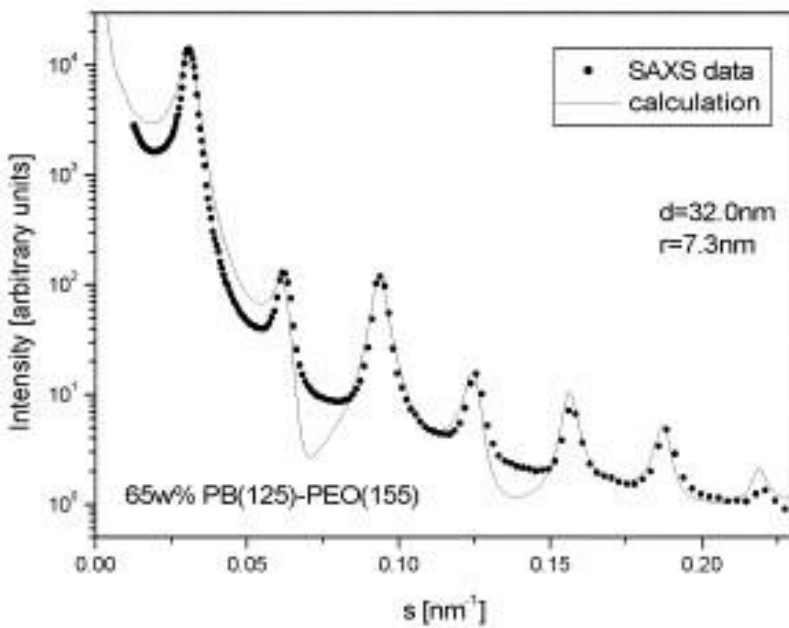
At high T thermal motion overcomes unfavourable interactions between blue and red segments



free energy = separation - stretching  
- interfacial energy

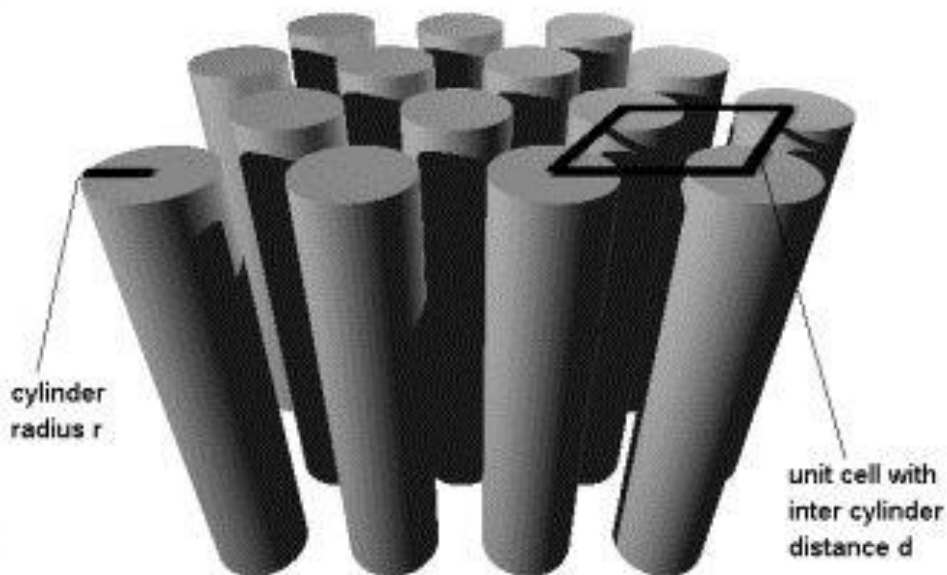
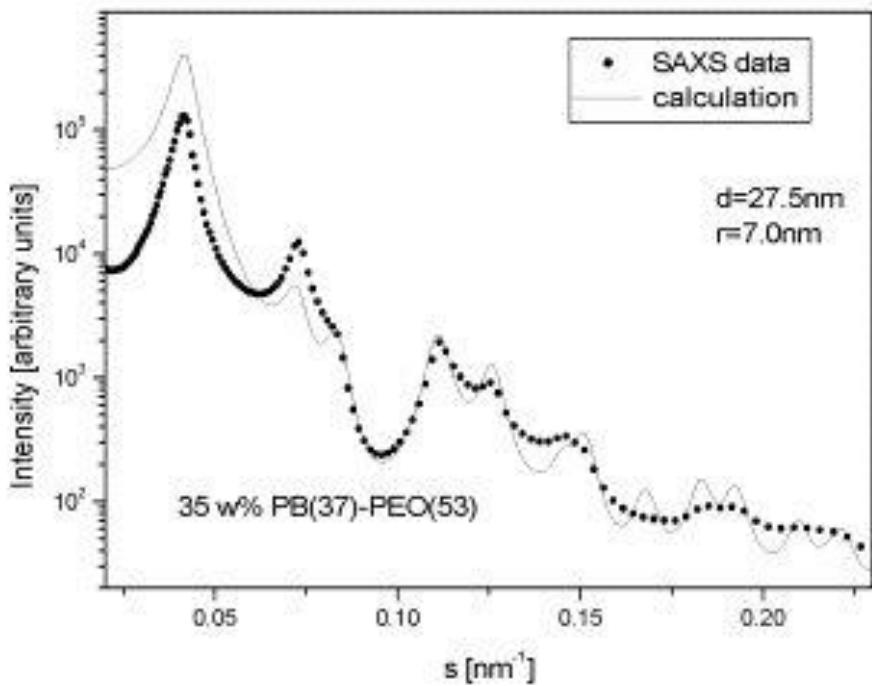


# Lamellar phase



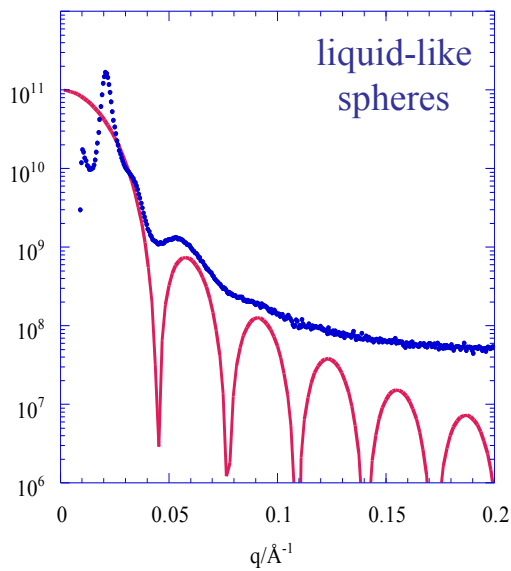
Peak order –  $q_0, 2q_0, 3q_0, 4q_0$

# Hexagonal phase

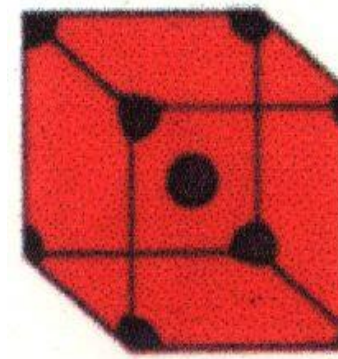
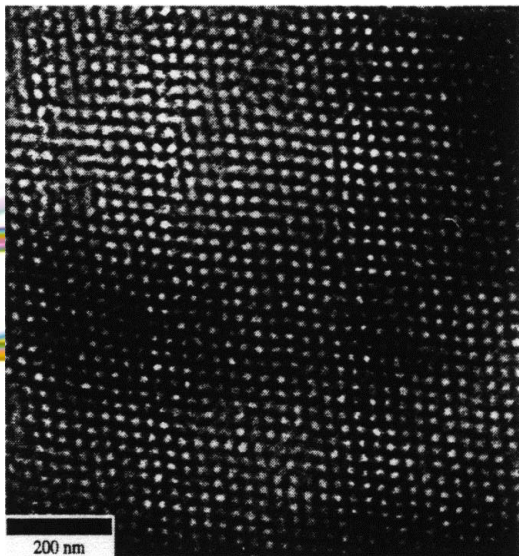
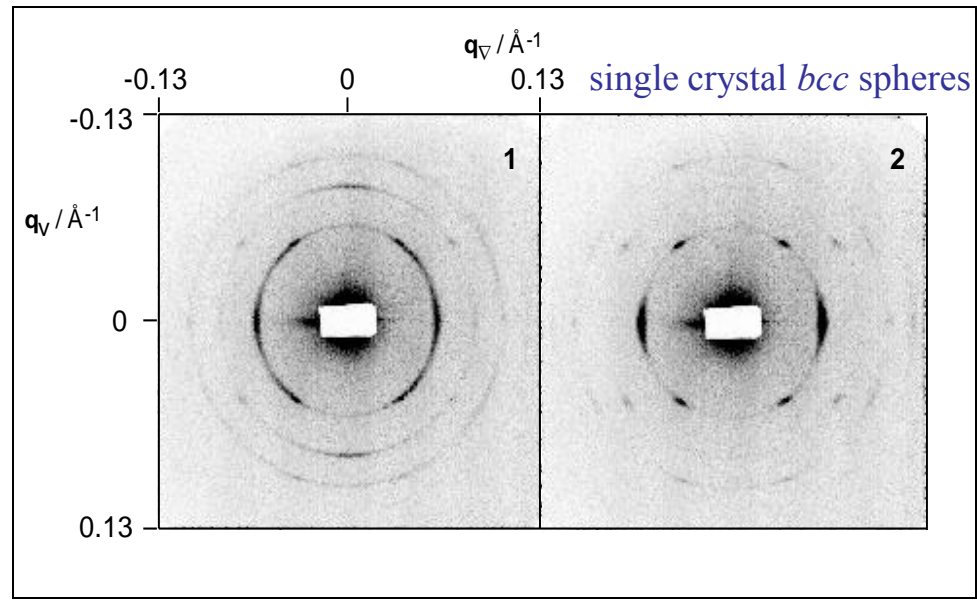


Hex Rods  $q_0 \sqrt{3}q_0 \sqrt{4}q_0$

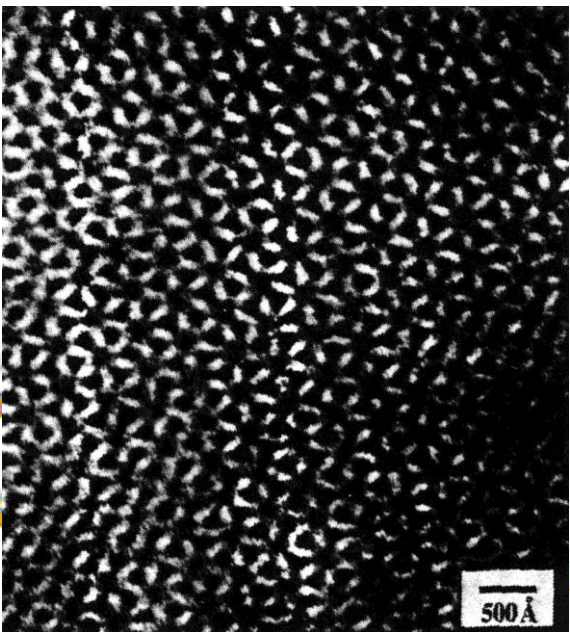
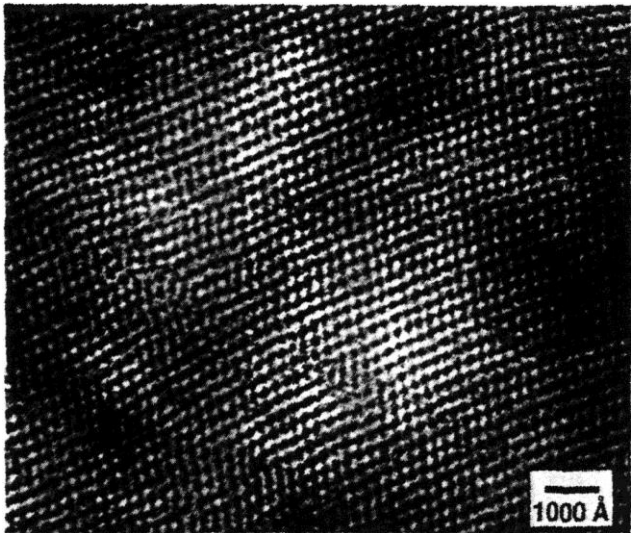
# Body Centred Cubic



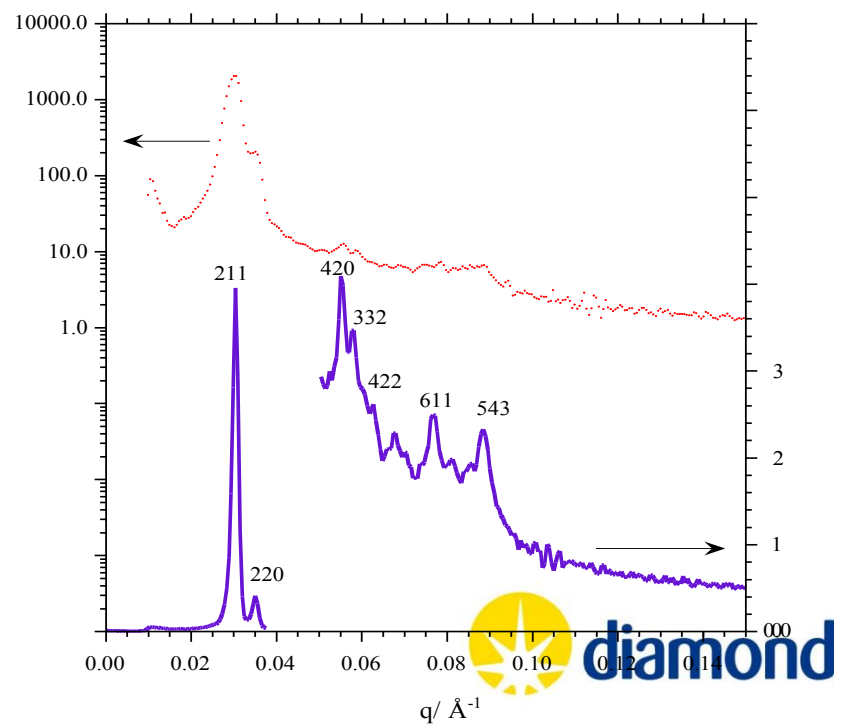
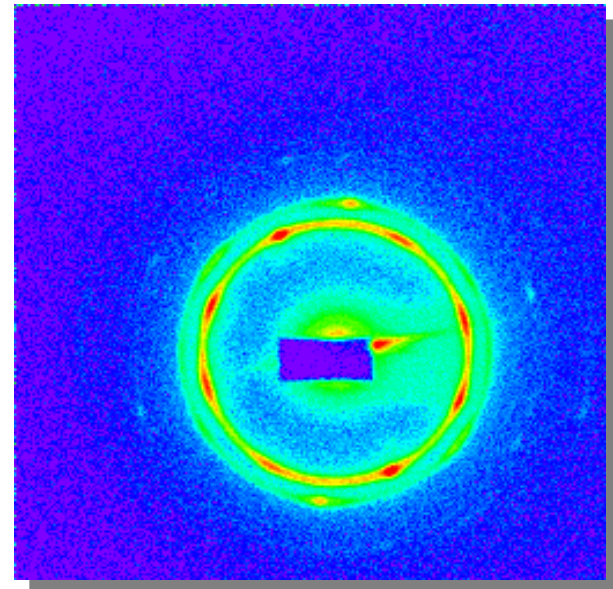
BCC Cubic  $q_0 \sqrt{2}q_0 \sqrt{3}q_0 \sqrt{4}q_0$



# Ia3d Gyroid

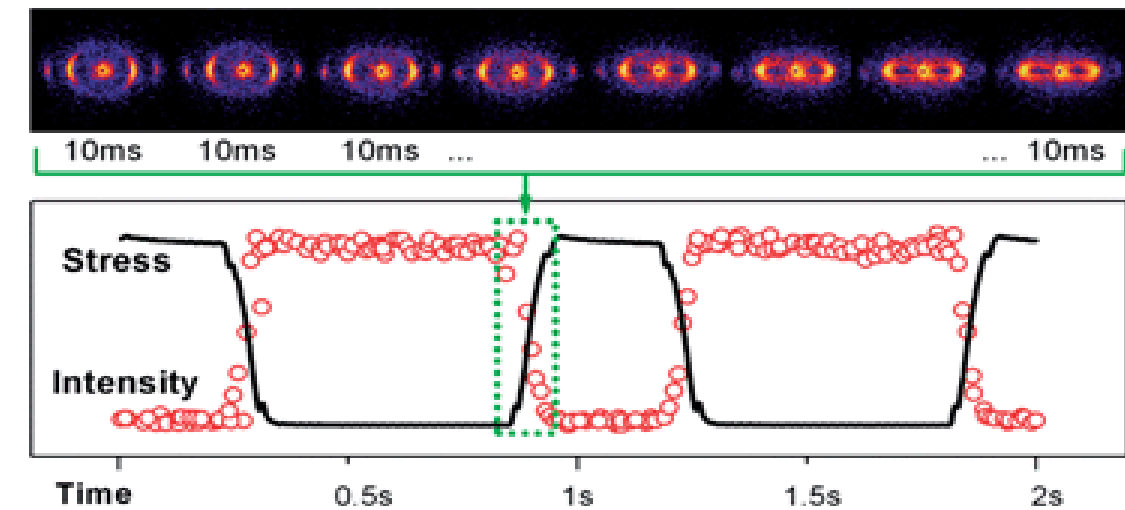
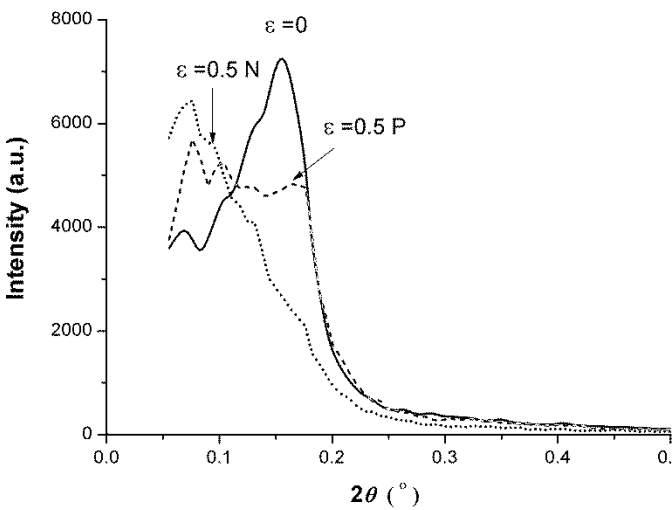


$\sqrt{6q_0}$   $\sqrt{8q_0}$   $\sqrt{14q_0}$   $\sqrt{16q_0}$   $\sqrt{20q_0}$   $\sqrt{22q_0}$



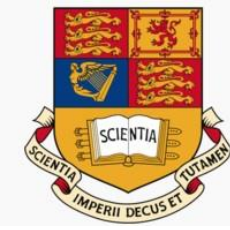


# A real time SAXS study of oriented block copolymers during fast cyclical deformation, with potential application for prosthetic heart valves

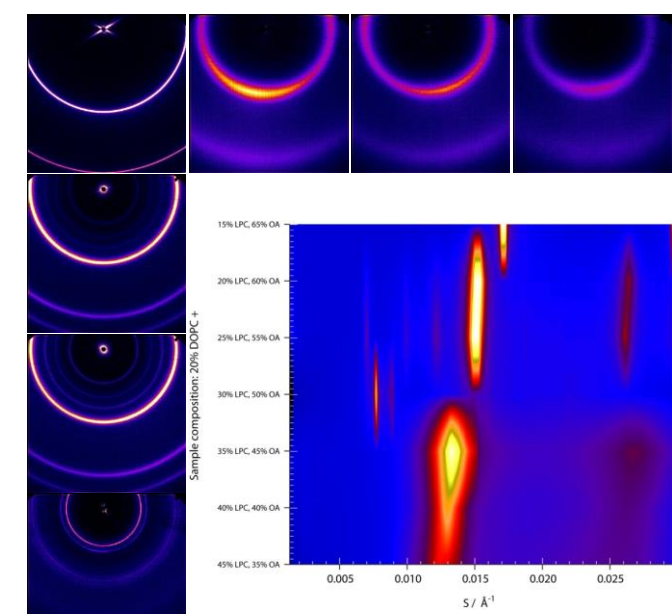
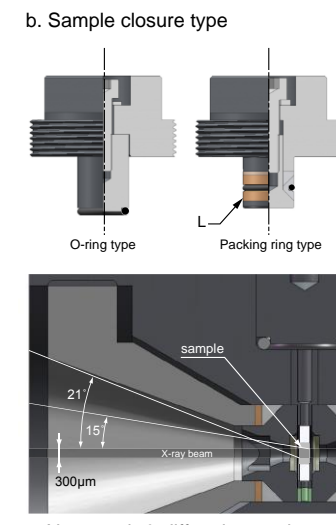
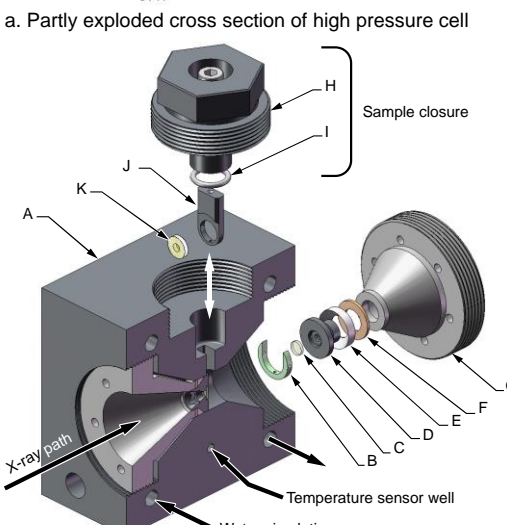
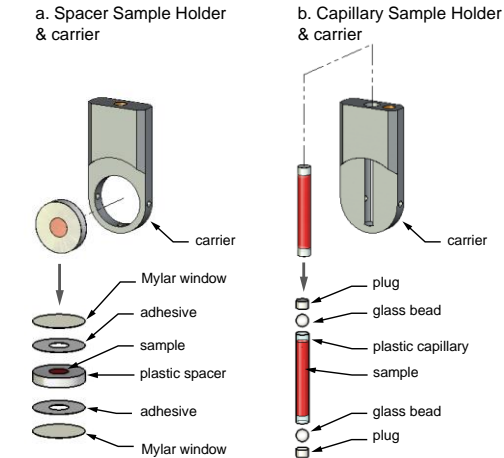
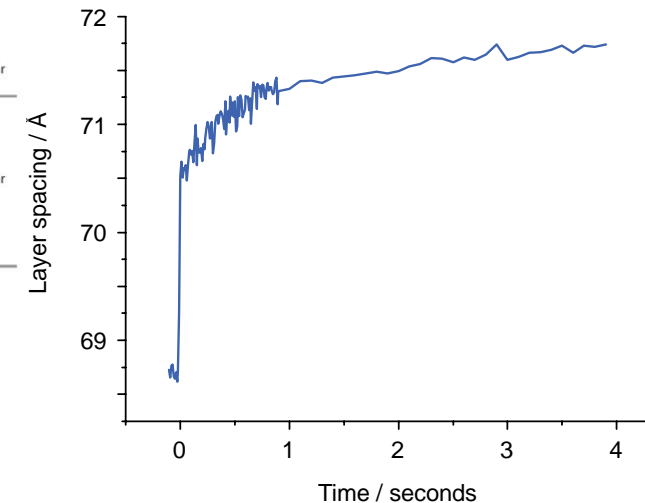
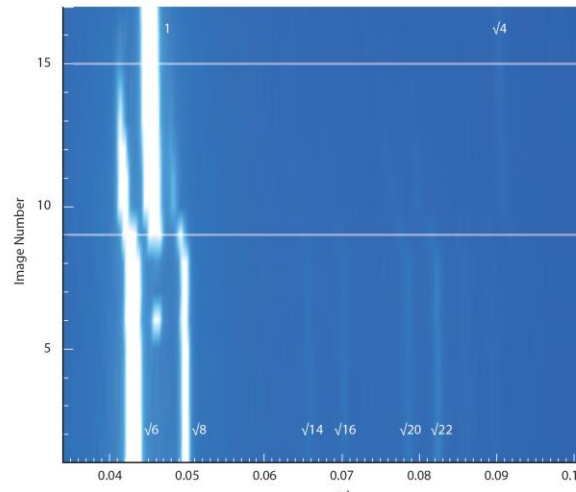


- Study of a range of thermoplastic elastomers with all rubbery components in the block copolymers
  - Time resolution of RAPID 10ms used (although trials of <1ms also proved successful)
  - Cycling used to mimic conditions for a prosthetic heat valve (10,000 cycles)



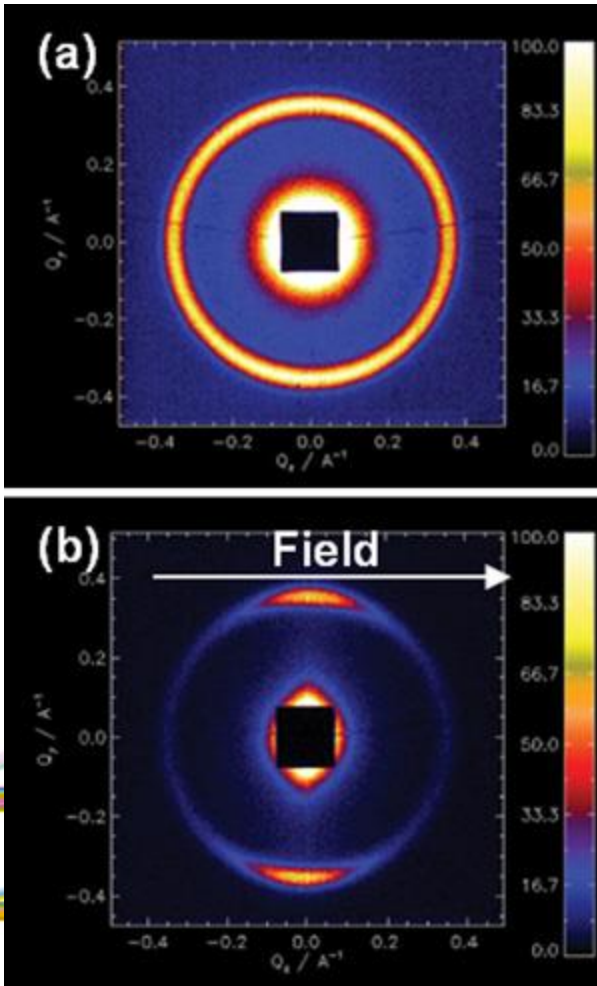


# Time resolved X-ray diffraction studies of drug induced membrane degradation

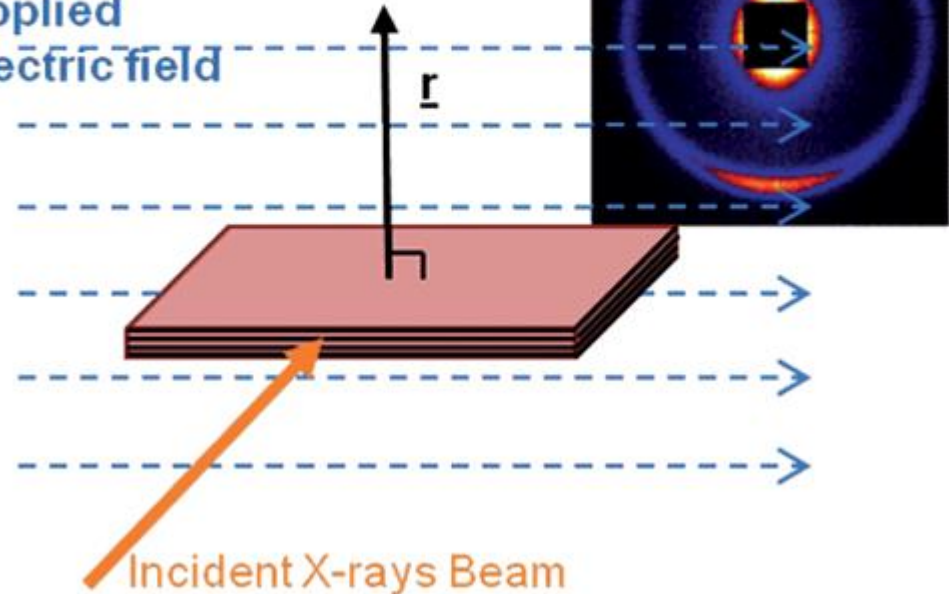




# Electric Field Induced Orientational Order in Suspensions of Anisotropic Nanoparticles



Applied  
electric field

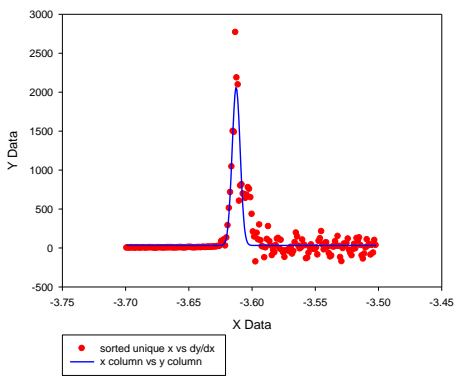


Scattering pattern obtained from Permanent Rubine in dodecane (30 wt%) using short camera length with (a) zero field (b) Electric field applied (4V=mm) giving nematic phase.

# Microfocus End Station

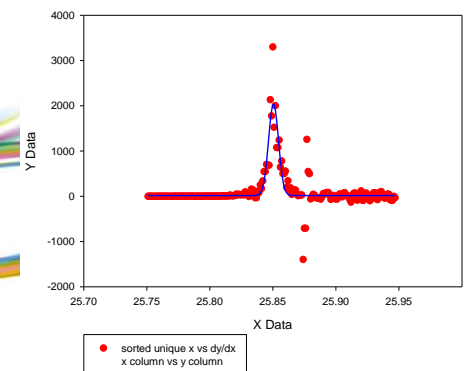
$$\text{FWHM}_h = 12.7 \mu\text{m}$$

$$f=y_0+a\cdot\exp(-.5\cdot((x-x_0)/b)^2)$$



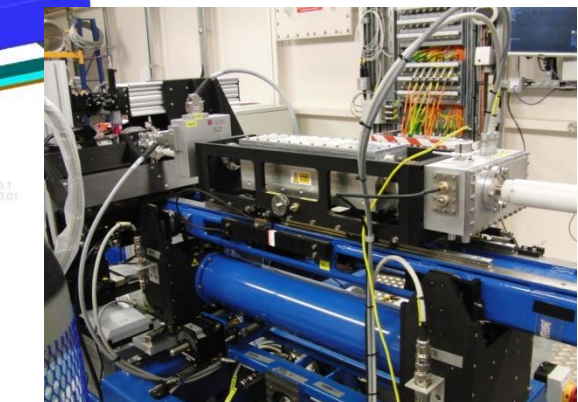
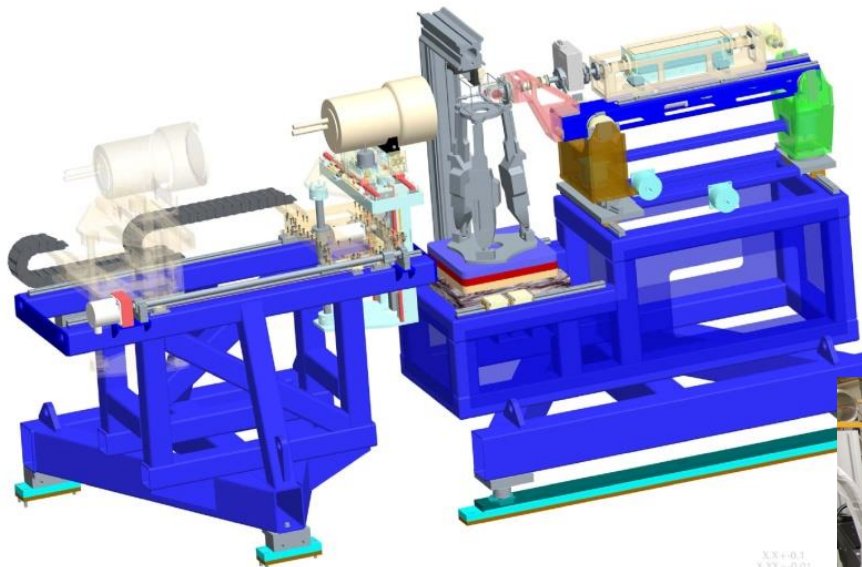
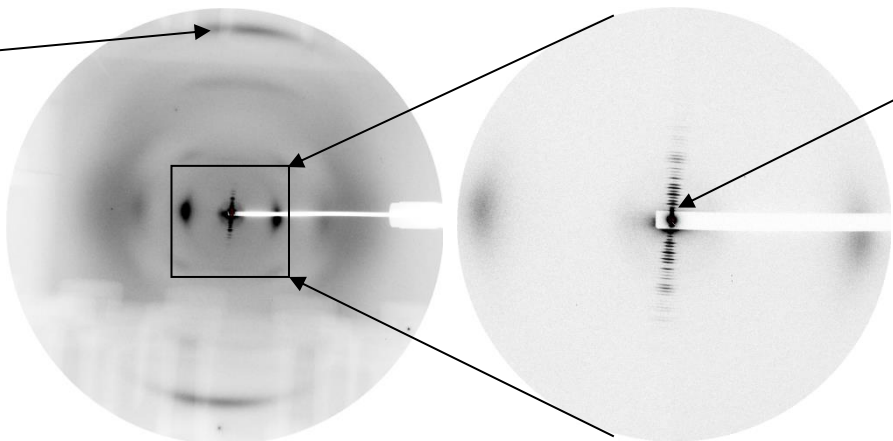
$$\text{FWHM}_v = 10.4 \mu\text{m}$$

$$f=y_0+a\cdot\exp(-.5\cdot((x-x_0)/b)^2)$$



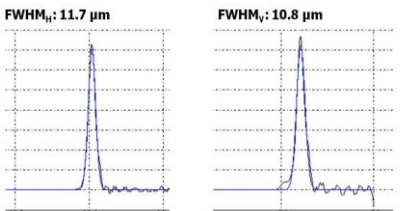
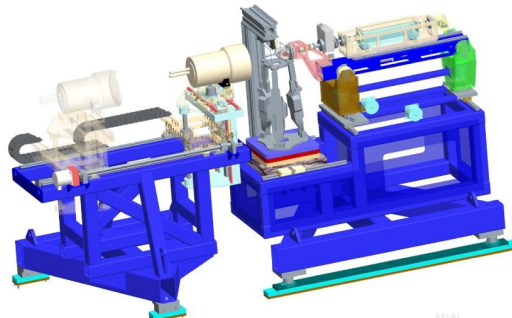
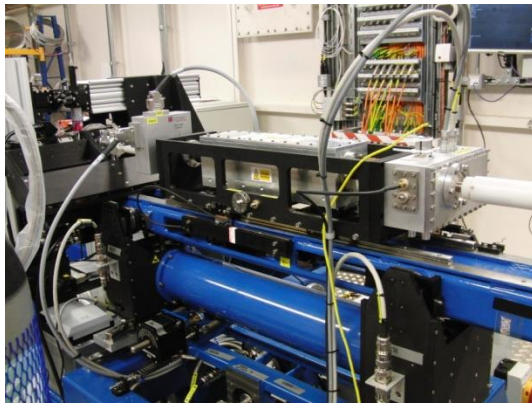
2.86 Å distance  
between amino  
acids in Type I  
collagen helix

650 Å first order  
of dry Type I  
collagen

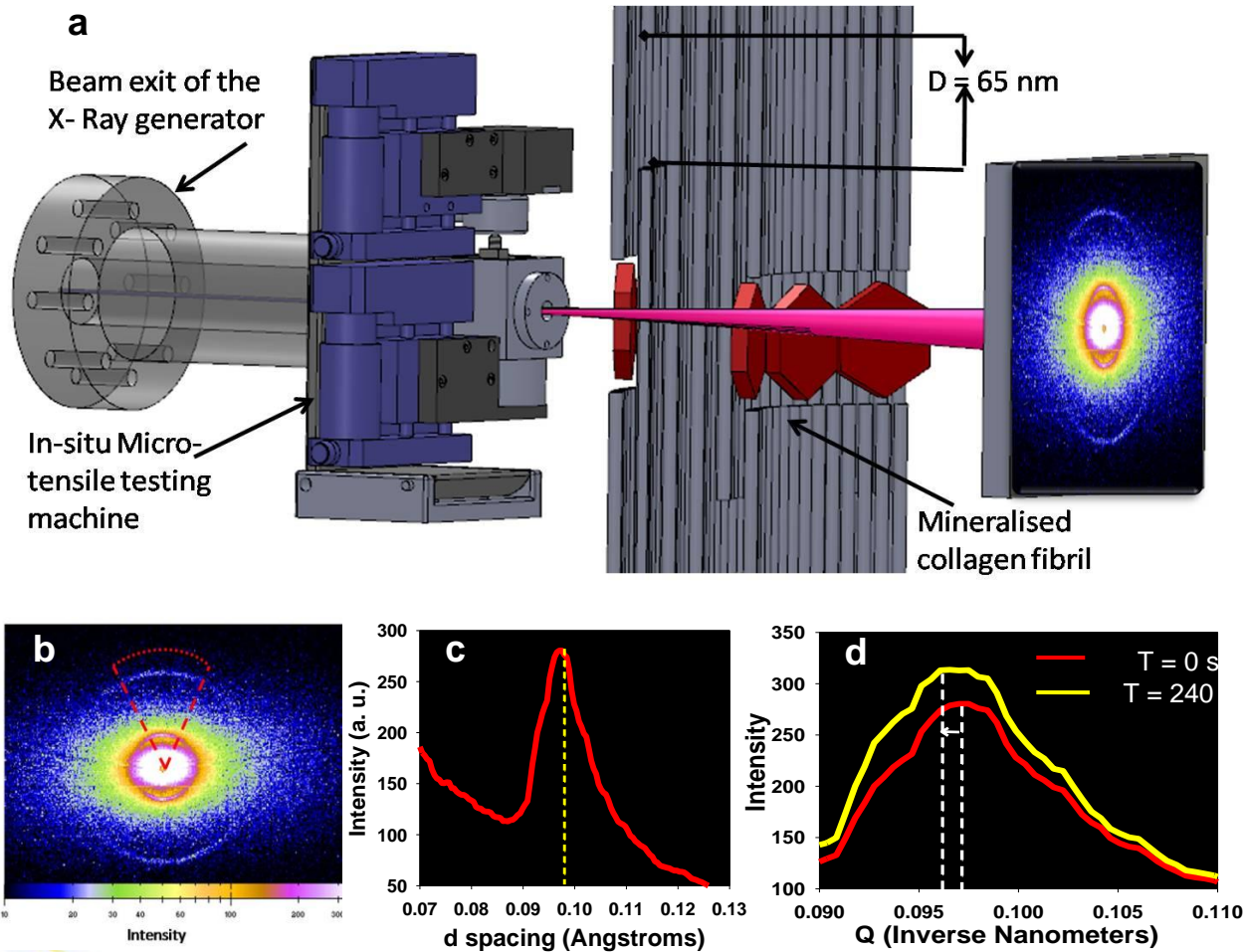




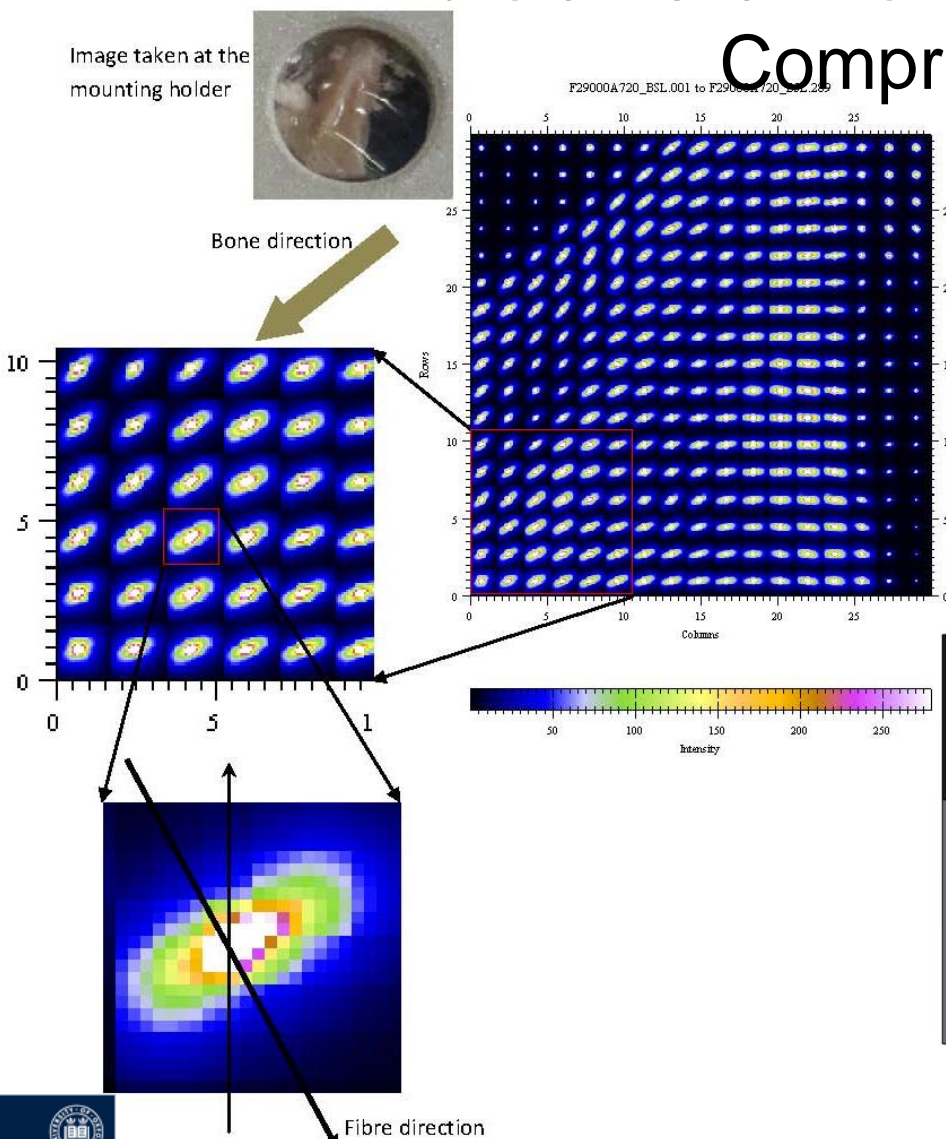
# Nanoscale Fracture Mechanisms in Fibrolamellar Bone in Bending and Compression



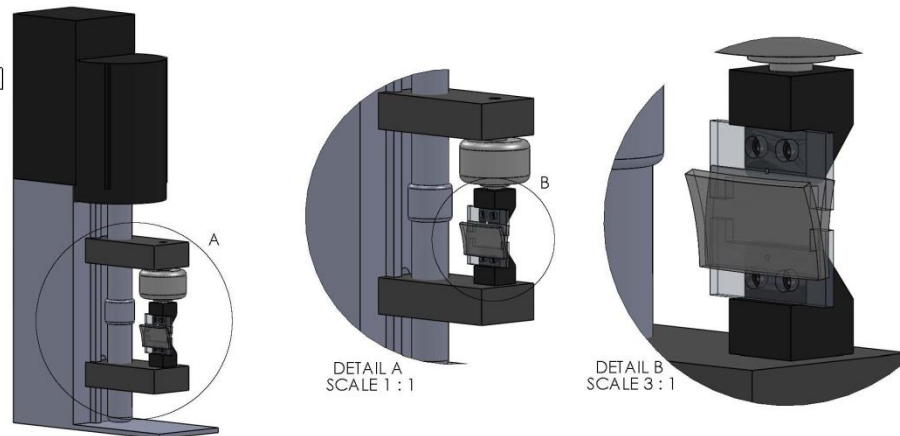
Microfocus spot obtained on I22 with CRL (90 lenses) at 14 keV



# Nanoscale Fracture Mechanisms in Fibrolamellar Bone in Bending and Compression

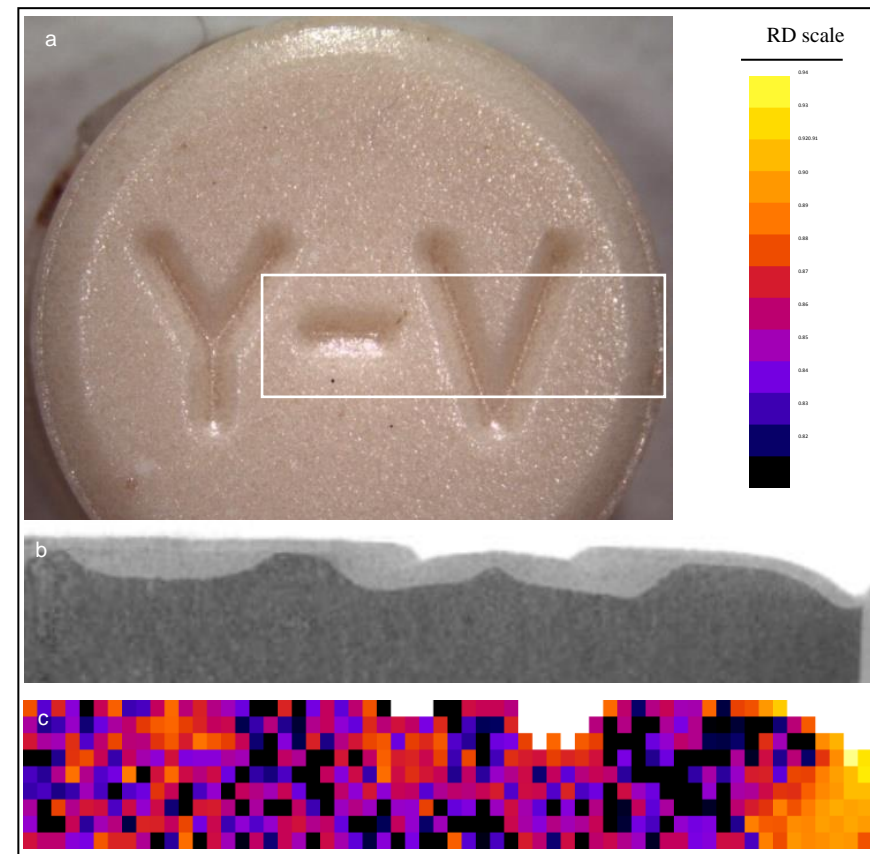
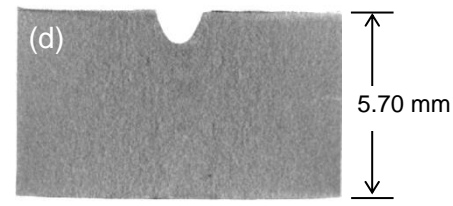
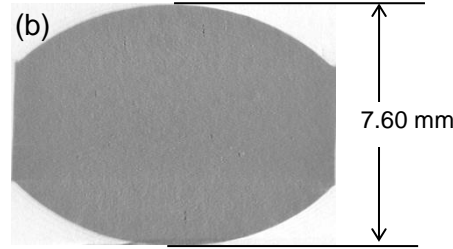
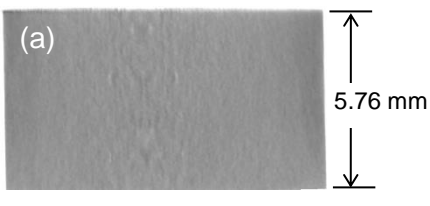


- Collagen Fibrillar strain
  - Micro damage and cracking
  - Mineral crystallite orientation

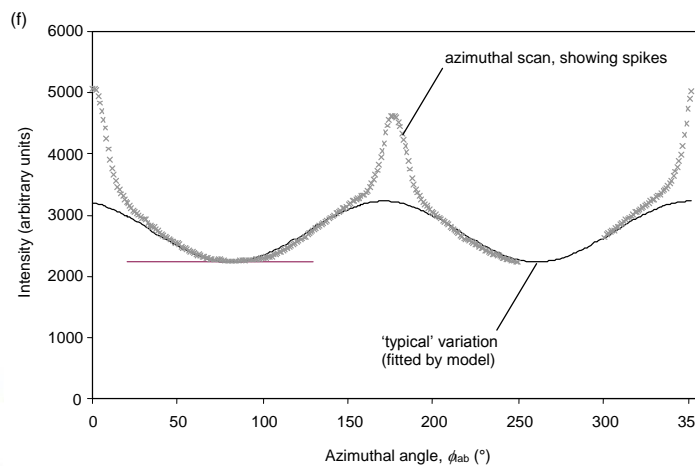
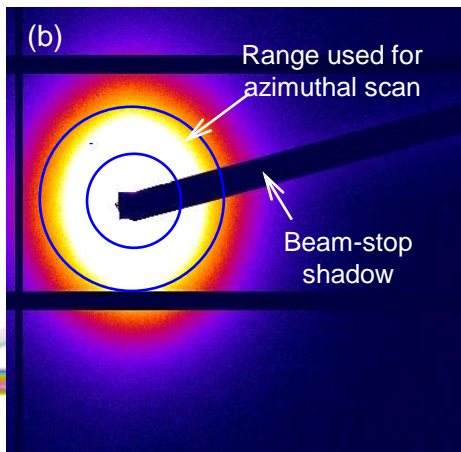
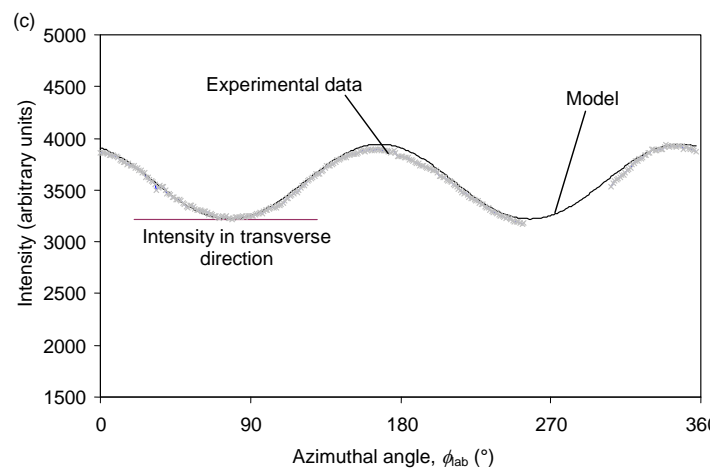
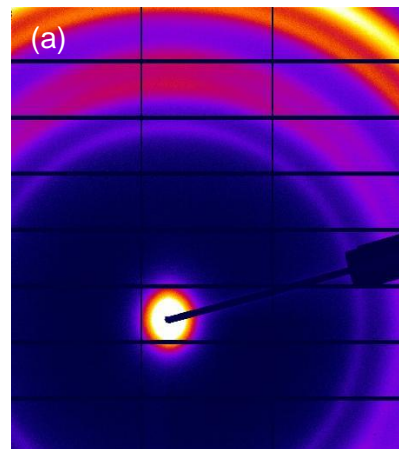


# Tablet Compaction and its effect on pharmaceutical activity

Tablet Test shapes including representative indentation types

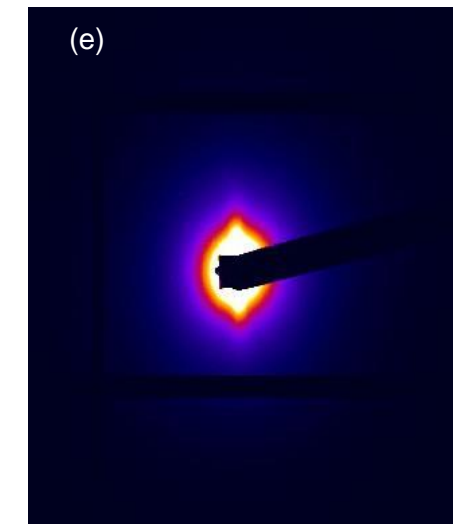
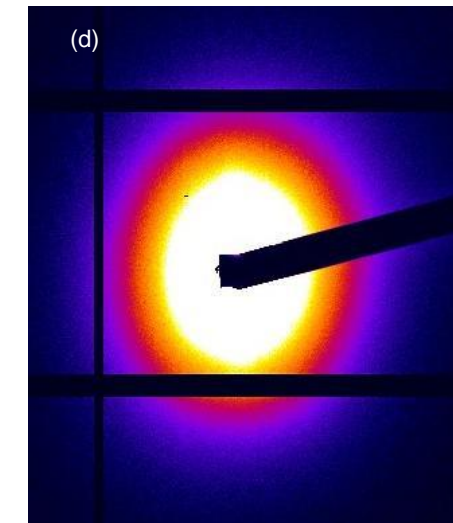


# Compaction/ Morphology

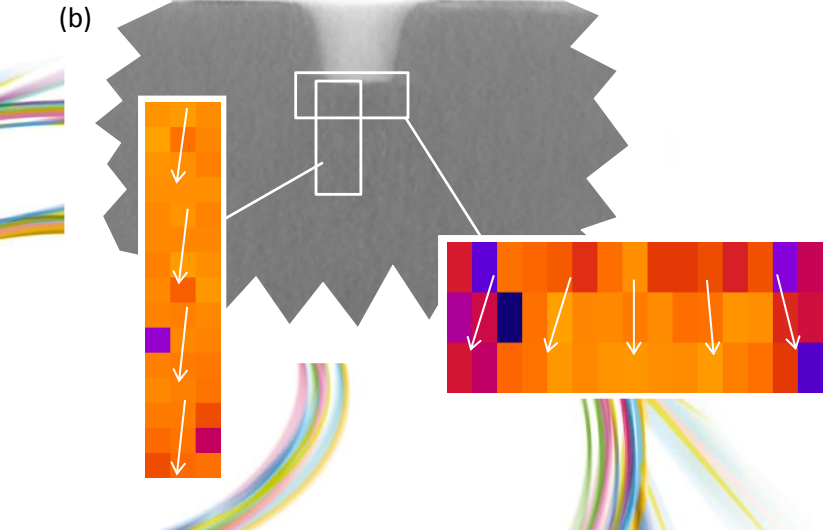
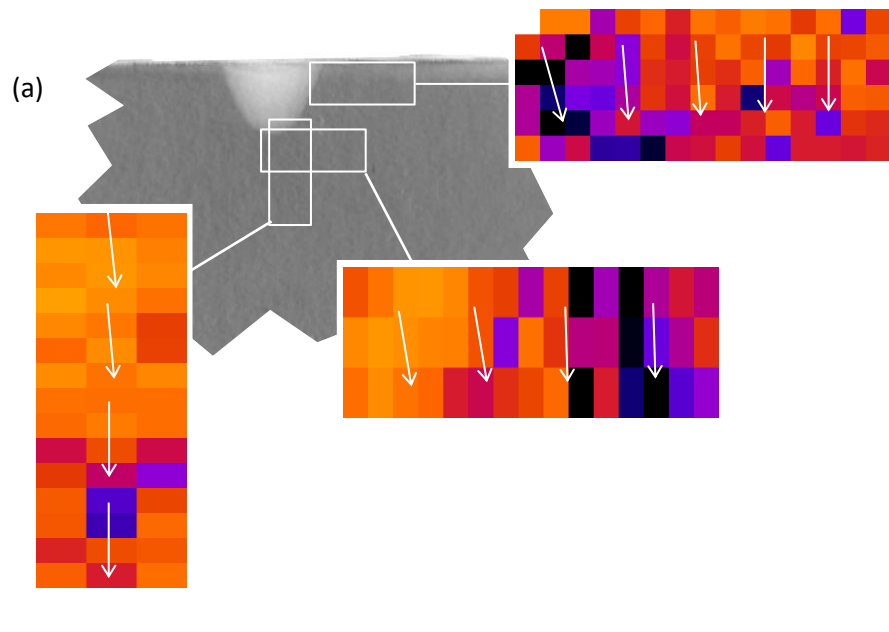


$$\langle \cos^2 \phi \rangle = \frac{\int_0^{180} I(\phi) \cdot \cos^2 \phi \cdot \sin \phi \cdot d\phi}{\int_0^{180} I(\phi) \cdot \sin \phi \cdot d\phi}$$

$$H = \frac{3\langle \cos^2 \phi \rangle - 1}{2}$$

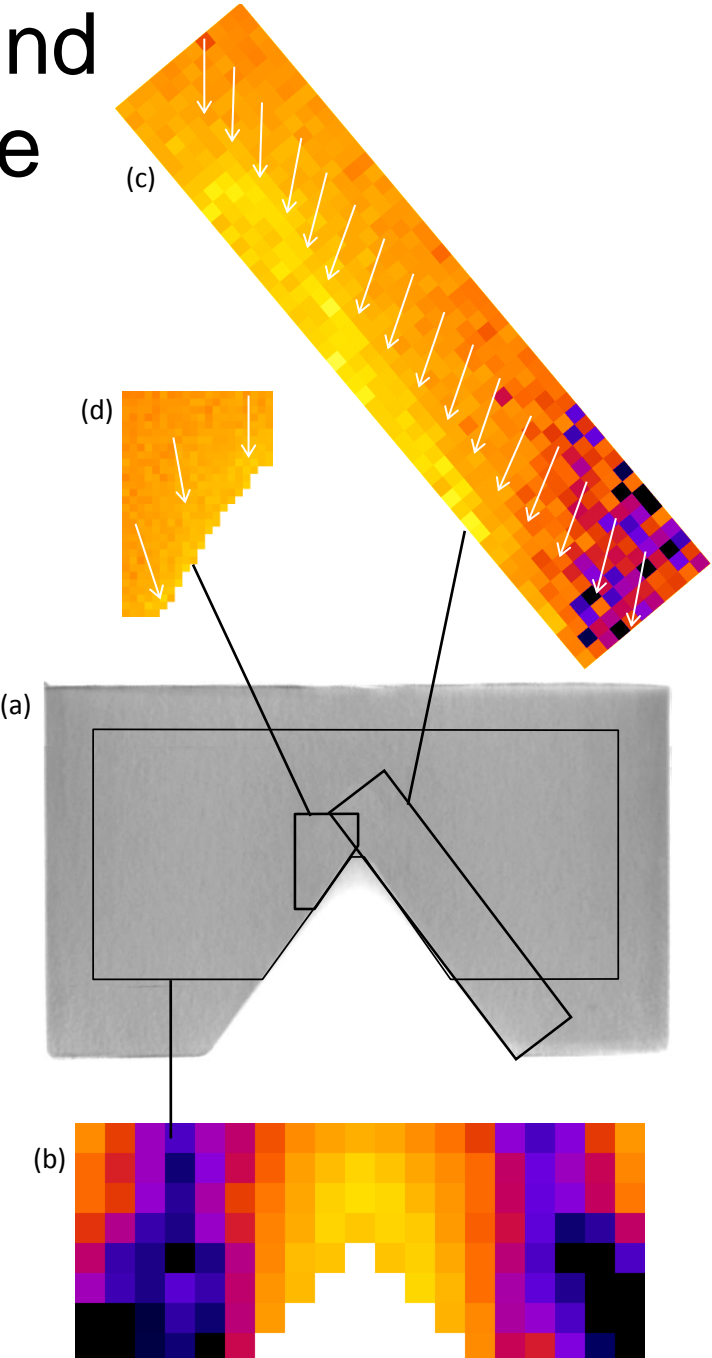


# Orientation around compaction site



Relative  
density

0.94
0.93
0.92
0.91
0.90
0.89
0.88
0.87
0.86
0.85
0.84
0.83
0.82



# Data Collection via GDA

The screenshot displays a multi-tiered interface for data collection at Diamond Light Source's Beamline I22. The top window is a 'Data Acquisition Client - Beamline I22 - 8.32.0' showing real-time monitoring of 'Live Waxs Data' and 'Live SxS Data'. It includes tabs for 'Setup', 'Ncd Status', 'Peak Fit Plot', and 'Edge Fit Plot'. Below these are sections for 'Saxs Peak', 'Waxs Peak', and 'Waxs Integrated'. The middle tier consists of three overlapping windows: 'Data Acquisition Client - Beamline I22 - 8.32.0' (top), 'Data Acquisition Client - Beamline I22 - 8.32.0' (middle), and 'Data Acquisition Client - Beamline I22 - 8.32.0' (bottom). The bottom window features a 'Python Console' tab with a script for 'samples-loop.py' which configures a ladder of capillaries for scanning. The right side of the interface shows a 'SAXS' data visualization, a 'Scan Plot 1' showing 'd4d1 / s2\_xplus' data, and a 'Queue - waiting' panel listing scans like 'Scan 137282 d4d1' and 'Scan 137277'. A status bar at the bottom indicates the user is 'Baton held not!' and shows the date and time as 'Mon 23 Sep, 17:28:02'. The bottom right corner features the Diamond logo.

```
#!/usr/bin/python
# This script will set up a run to collect data for a series of capillaries in a ladder.
# The centres of the capillaries need to be scanned first and input into the red values!
# ...
samples={}
samples["1"] = "-19.41"
samples["2"] = "-14.56"
samples["3"] = "10.44"
samples["4"] = "25.37"
samples["5"] = "40.34"
samples["6"] = "55.88"
samples["7"] = "70.34"
samples["8"] = "85.34"
samples["9"] = "100.34"
samples["10"] = "115.35"
samples["11"] = "130.34"
samples["12"] = "145.35"

print "Start collecting data"
# ...
pos poyy 77.56
pos basex 19.51
pos shutter "Open"
positions=samples.keys()
positions.sort()

for position in positions:
    sample=sample[position]
    print "Position "+position+" "+sample+" sample "+str(sample)
    finder.find("G4MDetector").setMetadataValue("title", sample+" "+str(position)+" "+basex+" "+position)
    pos basex
    pos shutter
    pause

pos shutter "Close"
pos poyy 22.56
pos basex 115.35
print "Script done"
```

# Data Reduction

Error Propagation

Axes Propagation

Normalisation

1D/2D



Detector Corrections

1D/2D



Background Subtractions

1D/2D



Absolute intensity

1D/2D



Radial Averaging

1D

$I_0/I_t$

Dark Current,  
Detector Response,  
etc.



Sample cell, Porod,  
amorphous (variable)



By Cross calibration  
or directly

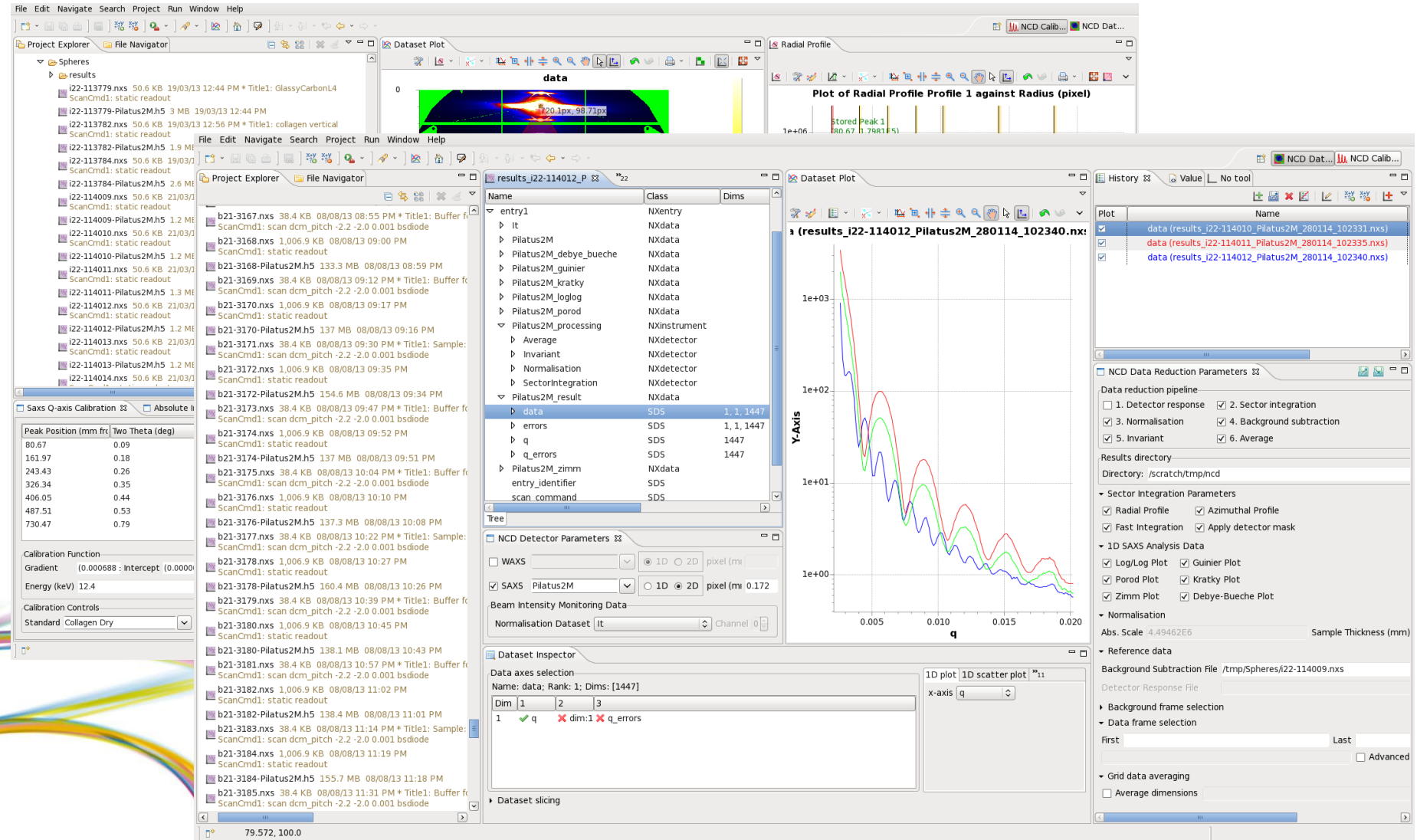


Sector and full  
circle with masking



diamond

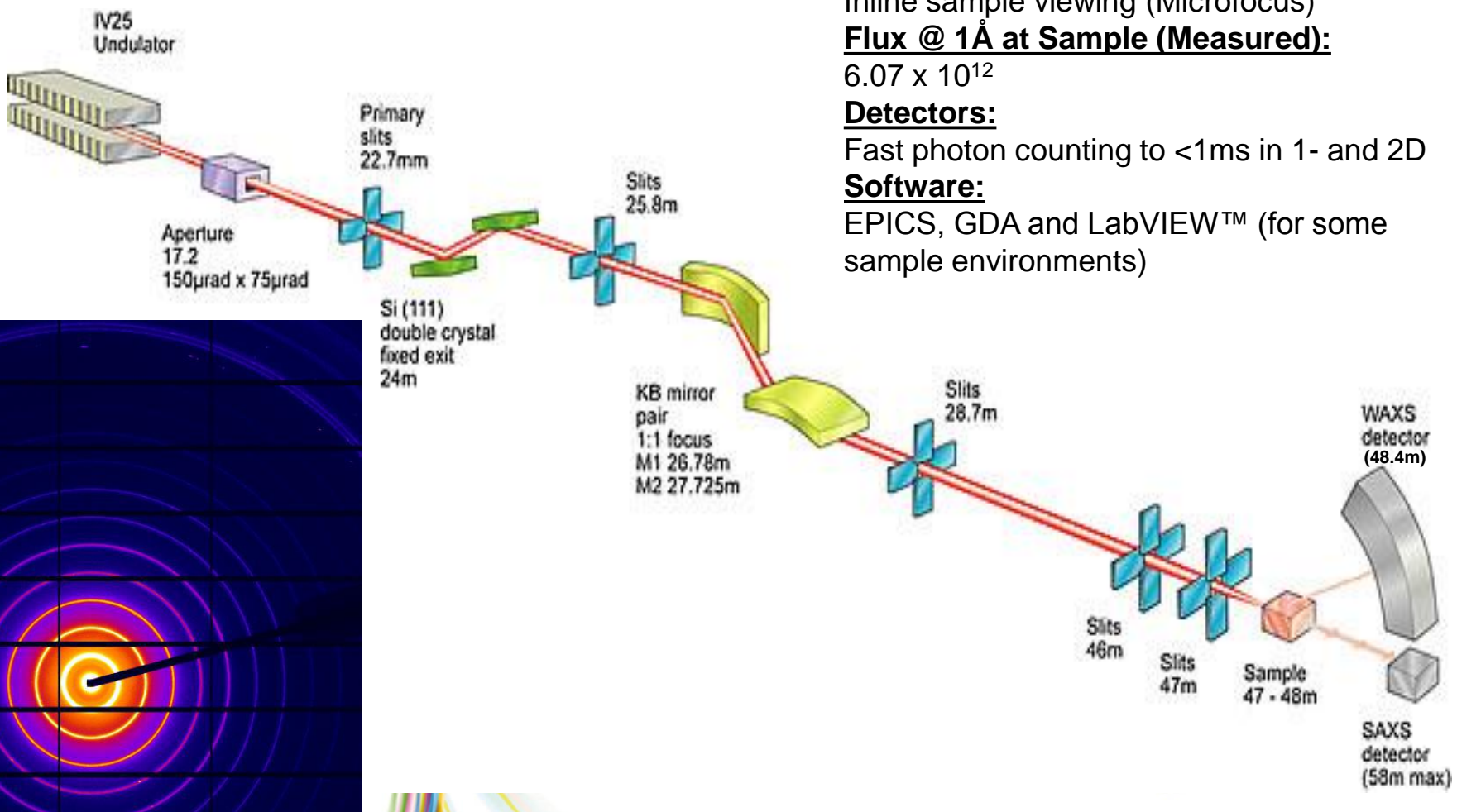
# Data Calibration & Reduction in Dawn



# Data Analysis

- Peaks and single parameter values are being integrated into DAWN.
- More detailed analysis is available *via* a range of packages that have been developed to focus on particular areas of science or experiment.

# I22 – Small Angle X-ray Scattering for Diamond



## Beamline:

Energy Range 3.7-20keV

d/ $\text{\AA}$  range 1-5000 $\text{\AA}$  (probably >1mm)

## Beam size:

70 $\mu\text{m}$  (V) – 330 $\mu\text{m}$ (H)

6 $\mu\text{m}$  x 7 $\mu\text{m}$  with microfocusing

## End Station:

Flexible Sample platform

Inline sample viewing (Microfocus)

## Flux @ 1 $\text{\AA}$ at Sample (Measured):

$6.07 \times 10^{12}$

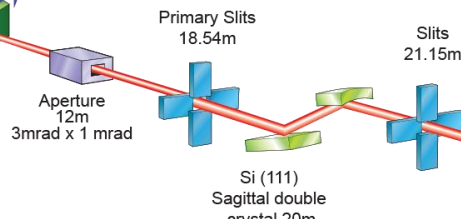
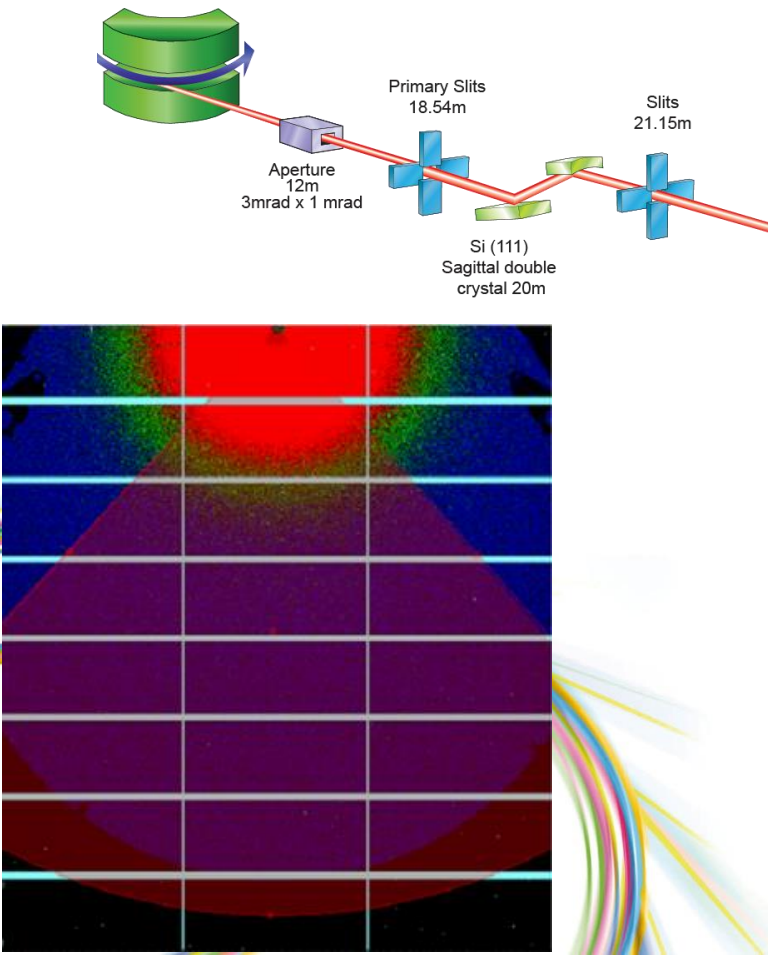
## Detectors:

Fast photon counting to <1ms in 1- and 2D

## Software:

EPICS, GDA and LabVIEW™ (for some sample environments)

# B21 – Solution SAXS for Diamond



## Beamline:

Energy Range 6-23keV  
d/Å range 1-2000Å

## Beam size:

250μm (V) – 350μm(H)

## End Station:

BioSAXS Robot for Solution Samples

## Flux @ 1Å at Sample (Measured):

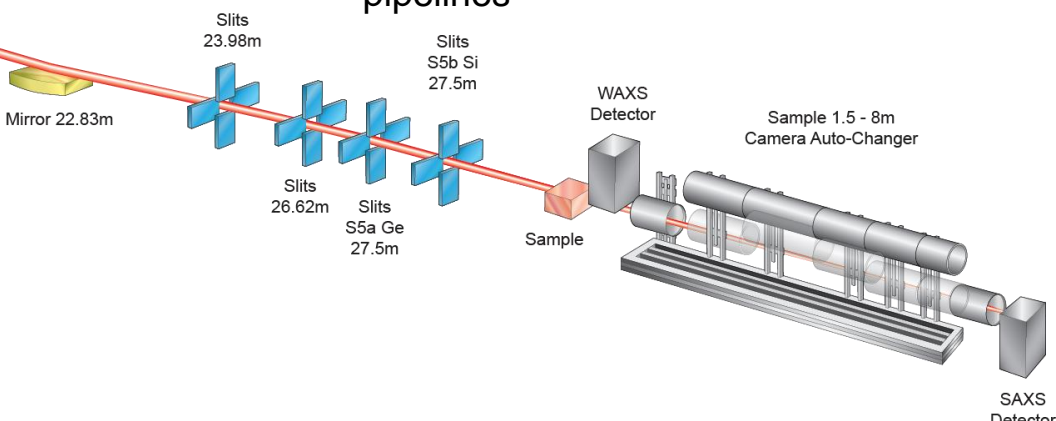
$8 \times 10^{11}$

## Detectors:

Fast photon counting to 30ms with P-2M

## Software:

EPICS, GDA and ISPyBB plus analysis pipelines



# Small Angle Scattering (SAXS)

- O. Glatter and O. Kratky – “Small Angle X-Ray Scattering” (<http://physchem.kfunigraz.ac.at/sm/Software.htm>)
- A. Guinier, G. Fournet, Chapman & Hall 1955- “Small Angle Scattering of X-Rays” (Good University Libraries!)
- L.A. Feigin and D.I. Svergun - “Structure Analysis by Small Angle X-Ray & Neutron Scattering” Nruka, Moscow, 1986, English Translation Ed. G.W. Taylor, Plenum, New York, 1987
- H. Brumberger – “Modern Aspects of Small Angle Scattering”, NATO ASI Series, Kluver Academic Press 1993
- P. Linder, Th Zemb - “Neutron, Xray & Light Scattering, Introduction to an Investigative tool for Colloidal and Polymeric Systems”
- Ryong-Joon Roe – “Methods of X-ray and Neutron Scattering in Polymer Science” Oxford University Press 2000
- Norbert Stribeck – “X-ray Scattering of Soft Matter” Springer 2007
- Wilfred Gille – “Particle and Particle Systems Characterisation” CRC Press 2014

Thanks for your attention

